PNAS
www.pnas.org

Supplementary Information for

Time-Restricted Feeding Protects the Blood Pressure Circadian Rhythm in Diabetic Mice

Tianfei Hou[a], Wen Su[a], Marilyn J. Duncan[b], Vsevolozhskaya A. Olga[c], Zhenheng Guo[a,d,1], and Ming C. Gong[e,1]

[a]Departments of Pharmacology and Nutritional Sciences, [b]Neuroscience, [c]Biotatistics, and [e]Physiology, University of Kentucky, Lexington, KY; [d]Research and Development, Lexington Veterans Affairs Medical Center, Lexington, KY, USA

[1]To whom correspondence may be addressed: Zhenheng Guo or Ming C. Gong

Email: zguo2@uky.edu or ming.gong@uky.edu

This PDF file includes:

Supplementary text (Material and Methods)

Figures S1 to S22

Tables S1

SI References

Material and Methods

Animals

Db/db and nondiabetic *db/+* mice (Stock No.: 000642) were purchased from the Jackson Laboratories (Bar Harbor, ME). All mice were fed with chow diet with free access to water and kept in a light-tight box under a 12:12 light: dark cycle. Male mice were used in the current study. All animal procedures were approved by the Institutional Animal Care and Use Committee of the University of Kentucky.

Feeding schedules

The mice were fed ALF (ad libitum), 8-h TRF (8 hours of food access from ZT13 to ZT21 [ZT0 is the time of lights-on, and ZT12 is the time of lights-off]), or 12-h TRF (12 hours of food access from ZT12 to ZT24) for the periods as described in the result and figure legends.

Food intake diurnal rhythm measurement

The food intake diurnal rhythm was comprehensively characterized by using a metabolic chamber (indirect gas calorimetry LabMaster system, TSE System, Bad Homburg, Germany) or a BioDAQ system (Research Diet, New Brunswick, NJ). The mice were acclimated to the systems for at least 7 days; then, the food intake was quantified continuously for a minimum of 3 consecutive days.

Telemetric measurement of the circadian rhythms of BP, heart rate, and locomotor activity

The mice were chronically instrumented in the left common carotid artery with a telemetry probe (TA11PA-C10, Data Sciences International, St. Paul, MN, USA) as described previously (1-3). After 7-10 days of recovery, systolic BP (SBP), diastolic BP (DBP), heart rate (HR), and locomotor activity were recorded for at least 3 consecutive days in home-caged conscious free-moving mice. The telemetric data were analyzed by Dataquest A.R.T. software (Data Sciences International [DSI], St. Paul, MN).

Metabolic characterizations of the animals

Body composition (lean mass and fat mass) was assessed by nuclear magnetic resonance NMR spectroscopy (Echo MRITM-100H, Houston, TX). Nonfasting blood glucose was measured by a StatStrip® XepressTM glucometer (NOVA® biomedical, Waltham, MA, USA). Respiratory exchange ratio (RER) and energy expenditure (EE) were measured using the metabolic chamber. Oxygen consumption and carbon dioxide production in the metabolic chambers were measured every 30 min for 3 consecutive days. RER and EE were calculated using the accompanying TSE PhenoMaster software.

Urinary and plasma catecholamines, aldosterone, and corticosterone measurement

The mice were acclimated in the metabolic cage (Tecniplast, S.p.A.) for about 12 hours, and then urine samples were collected in 6-h interval from ZT0 to 6, ZT6 to 12, ZT12 to 18, and ZT18 to 24 in *db/db* mice and in the 12-h interval from ZT0 to ZT12 and ZT12 to ZT24 in control mice. Plasma samples were collected at ZT6 during the light phase in *db/db* mice. The epinephrine, norepinephrine, and normetanephrine in urine or plasma were determined by the ELISA kits (Abnova, Taipei, Taiwan). The urinary aldosterone and corticosterone were determined by the ELISA kits from Enzo Life Sciences, Inc.

(Farmingdale, NY) and Arbor Assay (Ann Arbor, MI), respectively. Total contents of epinephrine, norepinephrine, normetanephrine, aldosterone, and corticosterone in the 6-h urine samples were calculated by concentrations × urine volumes.

Heart rate variability analysis

Heart rate variability was analyzed from the telemetry data by frequency domain and time domain methods using Ponemah Software (Data Sciences International; St. Paul, MN, version 6.32). For frequency domain analysis, 2 min segments at 20 min interval over 72 hours were selected and scanned to ensure they were free of artifacts. Each segment was interpolated to 20 Hz using the quadratic method. Subsequently, the data were subdivided into 50 overlapping series and computed by Fast Fourier Transform using the Hanning window method. The cut-off frequency range for low-frequency (LF) was 0.15-0.6 Hz, optimized by Baudrie's group (4). The high-frequency (HF) range was 1.5-4 Hz. For time-domain analysis, 5 min segments over 72 hours were calculated, and the root-mean-square successive beat-to-beat difference (rMSSD) was plotted as the marker of parasympathetic heart rate control. For both the frequency and time domain data, the heart rate variability was averaged in each correspondent hour over 3 days to generate the 24-h heart rate variability profile.

Baroreflex sensitivity analysis

The spontaneous baroreflex sensitivity was analyzed by sequence techniques using the Hemolab software (http://www.haraldstauss.com/HemoLab/HemoLab.html) as previously described (2). For every 1-h data, the software finds the sequences in which the systolic arterial pressure and pulse interval were positively correlated (r^2>0.80) and counts those

that contain at least four consecutive sequences as an effective Baroreflex. Baroreflex sensitivity was calculated as the average slope of the systolic pressure-pulse interval relationships with an auto threshold at 3 beats in delay. For each mouse, a total of 72 hourly baroreflex sensitivity data points were calculated from the 3 consecutive days of BP data and then averaged to generate one 24-h profile. For *db/db*-TRF group, 2 out of the 144 data points were excluded as they are identified as outliers by an outlier calculator (https://www.miniwebtool.com/outlier-calculator/).

Assessment of the prazosin-induced BP drop

Baseline BP was collected from 18-21 week-old control, *db/db*-ALF or *db/db*-TRF (2 weeks) mice at ZT 5 or ZT17 for one h. Then an α1-adrenergic receptor antagonist, prazosin, was injected (i.p., 1 mg/kg body weight), and BP data was collected for an additional 2 hours. The average BP in the one h prior to prazosin injection and the lowest BP after prazosin injection was selected to quantify the BP responses to prazosin.

Quantitative analysis of mRNA expression

The 21-week-old db/db and control mice were fed TRF or ALF for 4 weeks and then euthanized at ZT5, 11, 17, and 23. The liver, mesenteric arteries (MA), kidney, heart, and adrenal gland were collected in RNAlater solution. The fat surrounding the MA was carefully removed under a microscope. The mRNA levels of various clock genes were quantified by real-time PCR, as previously described (5). The real-time PCR primers for each gene were described in Table S1.

Cosinor analysis of Circadian rhythm

The amplitude, robustness, and acrophase of the circadian rhythms in MAP, SBP, DBP, HR, and locomotor activity were determined by the cosinor analysis software (Circadian Physiology, Second Edition, Dr. Robero Refinetti).

Statistical analysis

All data were expressed as mean ± SEM. The sample size was described in the figures and figure legends as biological replicates. For comparison of 1 parameter between 2 groups of mice, 2-tail Student's t-test was used. For comparison of 1 parameter between more than 2 groups of mice, one-way ANOVA with Tukey's post-test was used. For comparison of two parameters between ≥2 groups of mice, two-way ANOVA with Bonferroni's or Tukey's post-test as recommended by the software were performed. For comparison of three parameters between ≥2 groups of mice, three-way ANOVA with Tukey's post-test was performed. All statistical analysis was performed by Prism 8 software (GraphPad Software, San Diego, CA). $P < 0.05$ was defined as statistically significant.

SI References

1. Su W*, et al.* (2008) Hypertension and disrupted blood pressure circadian rhythm in Type 2 diabetic db/db mice. *Am J Physiol Heart Circ Physiol* 295(4):H1634-1641.

2. Xie Z*, et al.* (2015) Smooth-muscle BMAL1 participates in blood pressure circadian rhythm regulation. *J Clin Invest* 125(1):324-336.

3. Hou T, Su W, Guo Z, & Gong MC (2019) A Novel Diabetic Mouse Model for Real-Time Monitoring of Clock Gene Oscillation and Blood Pressure Circadian Rhythm. *J Biol Rhythms* 34(1):51-68.

4. Baudrie V, Laude D, & Elghozi JL (2007) Optimal frequency ranges for extracting information on cardiovascular autonomic control from the blood pressure and pulse interval spectrograms in mice. *Am J Physiol Regul Integr Comp Physiol* 292(2):R904-912.

5. Guo Z*, et al.* (2005) COX-2 up-regulation and vascular smooth muscle contractile hyperreactivity in spontaneous diabetic db/db mice. *Cardiovasc Res* 67(4):723-735.

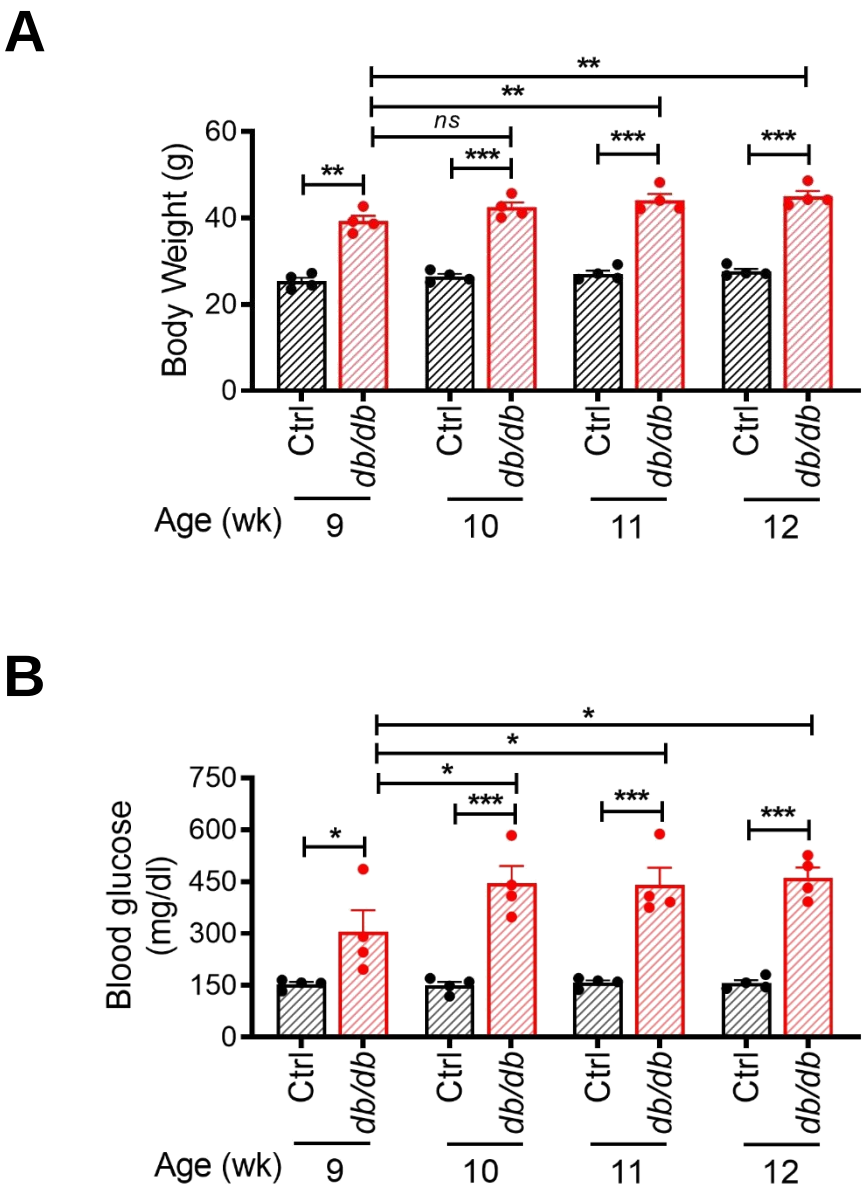

Fig. S1. Time course of body weight and nonfasting blood glucose in *db/db* and control mice. Body weight (**A**) and nonfasting blood glucose (**B**) in 9-, 10-, 11-, and 12-week-old type 2 diabetic *db/db* mice and age-matched nondiabetic control mice (*db/+*). The data were analyzed by 2-way ANOVA with multiple comparisons test and were expressed as the mean ± standard error (SEM). . *, p<0.05; **, p<0.01; ***, p<0.001; ns, not significant.

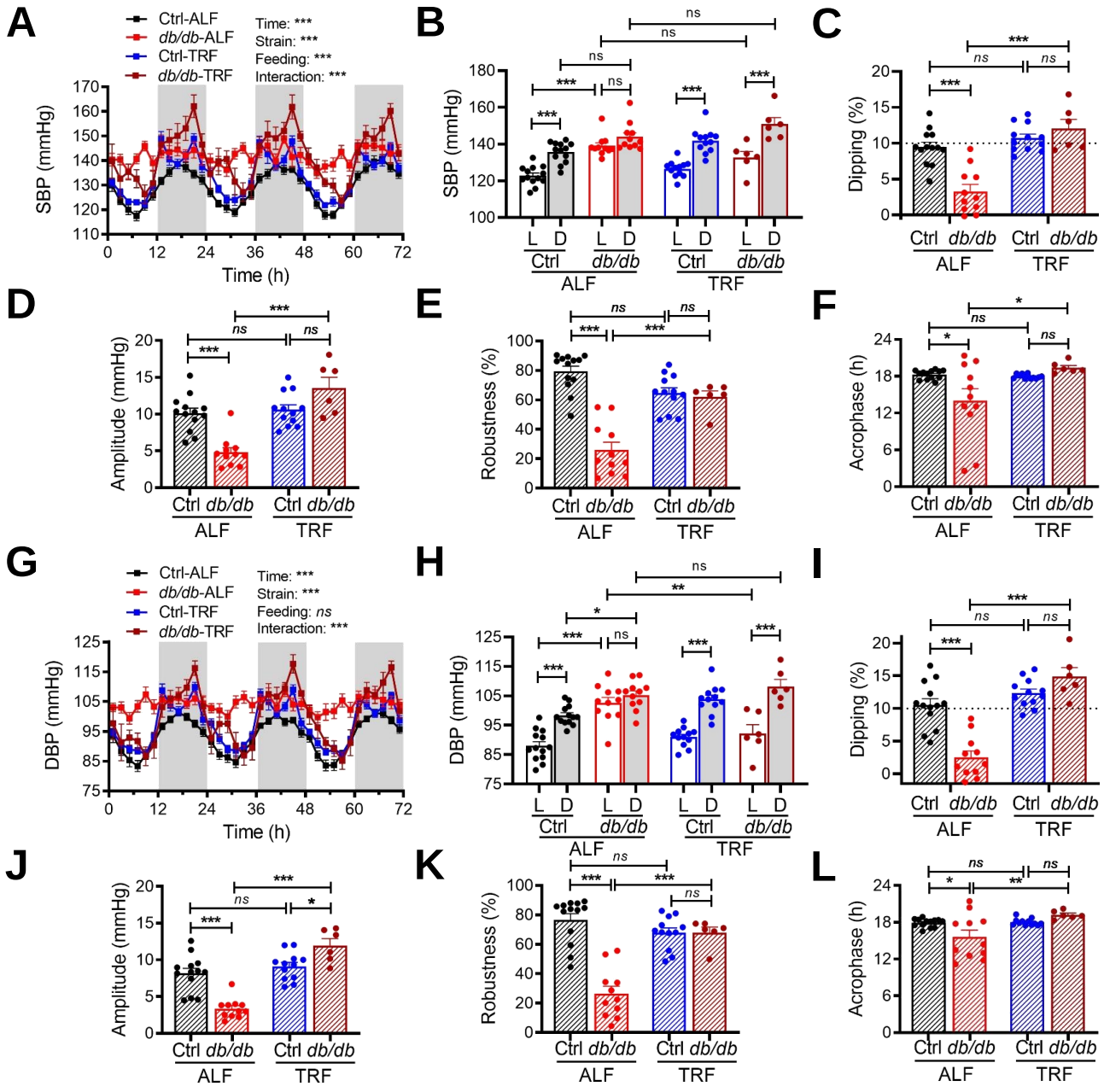

Fig. S2. Time-restricted feeding (TRF) protects *db/db* mice from systolic blood pressure (SBP) and diastolic blood pressure (DBP) nondipping. Six-week-old *db/db* and control (*db/+*) mice were fed *ad libitum feeding* (ALF) or 8-h TRF for 10 weeks. Blood pressure was recorded 10 weeks after ALF or TRF when mice were 16 weeks of age. (**A** and **G**) Daily profiles of SBP (A) and DBP (G) in 2-h interval over 72 h in Ctrl-ALF (n=13), Ctrl-TRF (n=12), *db/db*-ALF (n=11), and *db/db*-TRF (n=6) mice. The grey box indicates the dark phase. (**B** and **H**) The 12-h average SBP (B) and DBP (H) during the light (L) and dark (D) phase. (**C** and **I**) SBP (C) and DBP (I) dipping. The dashed line indicates 10% dipping. (**D** and **J**) Amplitude of the SBP (D) and DBP (J) circadian rhythms. (**E** and **K**) Robustness of the SBP (E) and DBP (K) circadian rhythms. (**F** and **L**) Acrophase of the SBP (F) and DBP (L) circadian rhythms. The data were analyzed by 3-way ANOVA (A, B, G, and H) and 2-way ANOVA (C–F and I–L) with multiple comparisons test and were expressed as the mean ± standard error (SEM). *, p<0.05; **, p<0.01; ***, p<0.001; ns, not significant.

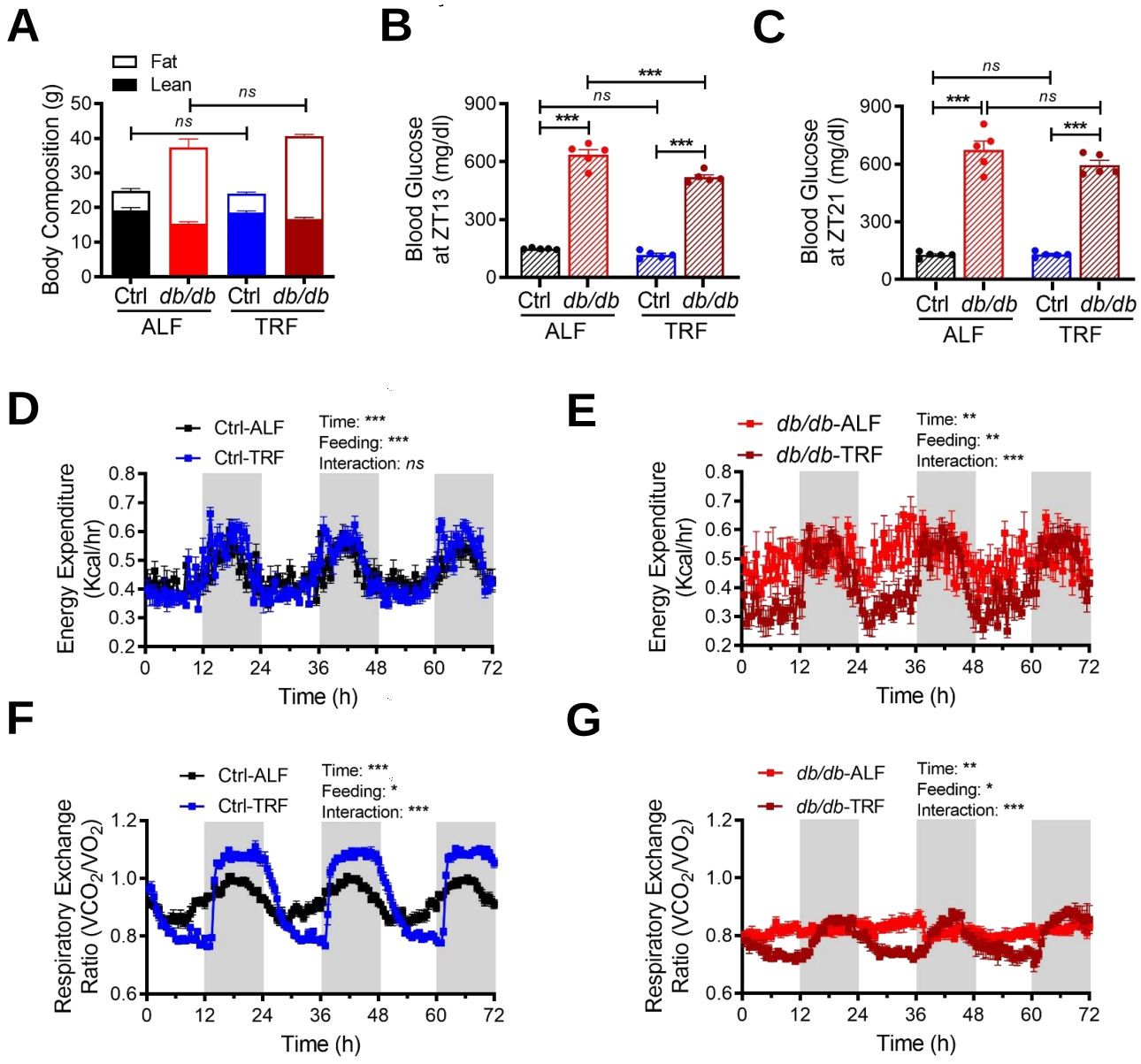

Fig. S3. Effects of TRF on body composition, blood glucose, energy expenditure, and respiratory exchange ratio in *db/db* mice. (**A**) Body composition (lean mass and fat mass) was measured by nuclear magnetic resonance spectroscopy in 14-week-old *db/db* and control (*db/+*) mice (5 mice/group) that had been fed under ALF or 8-hour (h) TRF for 8 weeks. (**B** and **C**) Nonfasting blood glucose was measured at ZT13 (B) and ZT21 (C) after 7-8 weeks of 8-h ALF or TRF. ZT, zeitgeber time (ZT0 = lights-on and ZT12 = lights-off). (**D**) Daily profiles of the energy expenditure (EE) in 0.5-h interval over 72 h in Ctrl-ALF mice (n=10) and Ctrl-TRF mice (n=10). (**E**) Daily profiles of EE 0.5-h interval over 72 h in *db/db*-ALF mice (n=5) and *db/db*-TRF mice (n=6). (**F**) Daily profiles of the respiratory exchange ratio (RER) in 0.5-h interval over 72 h in Ctrl-ALF mice (n=10) and Ctrl-TRF mice (n=10). (**G**) Daily RER profiles in 0.5-h interval over 72 h in *db/db*-ALF mice (n=5) and *db/db*-TRF mice (n=6). The EE and RER were measured by indirect calorimetry in the 16-18-week-old *db/db* and control (*db/+*) mice that had been fed ALF or 8-hour TRF for 10 to 12 weeks. The grey box indicates the dark phase. The data were analyzed by 2-way ANOVA with multiple comparisons test and were expressed as the mean ± standard error (SEM). *, $p<0.05$; **, $p<0.01$; ***, $p<0.001$; ns, not significant.

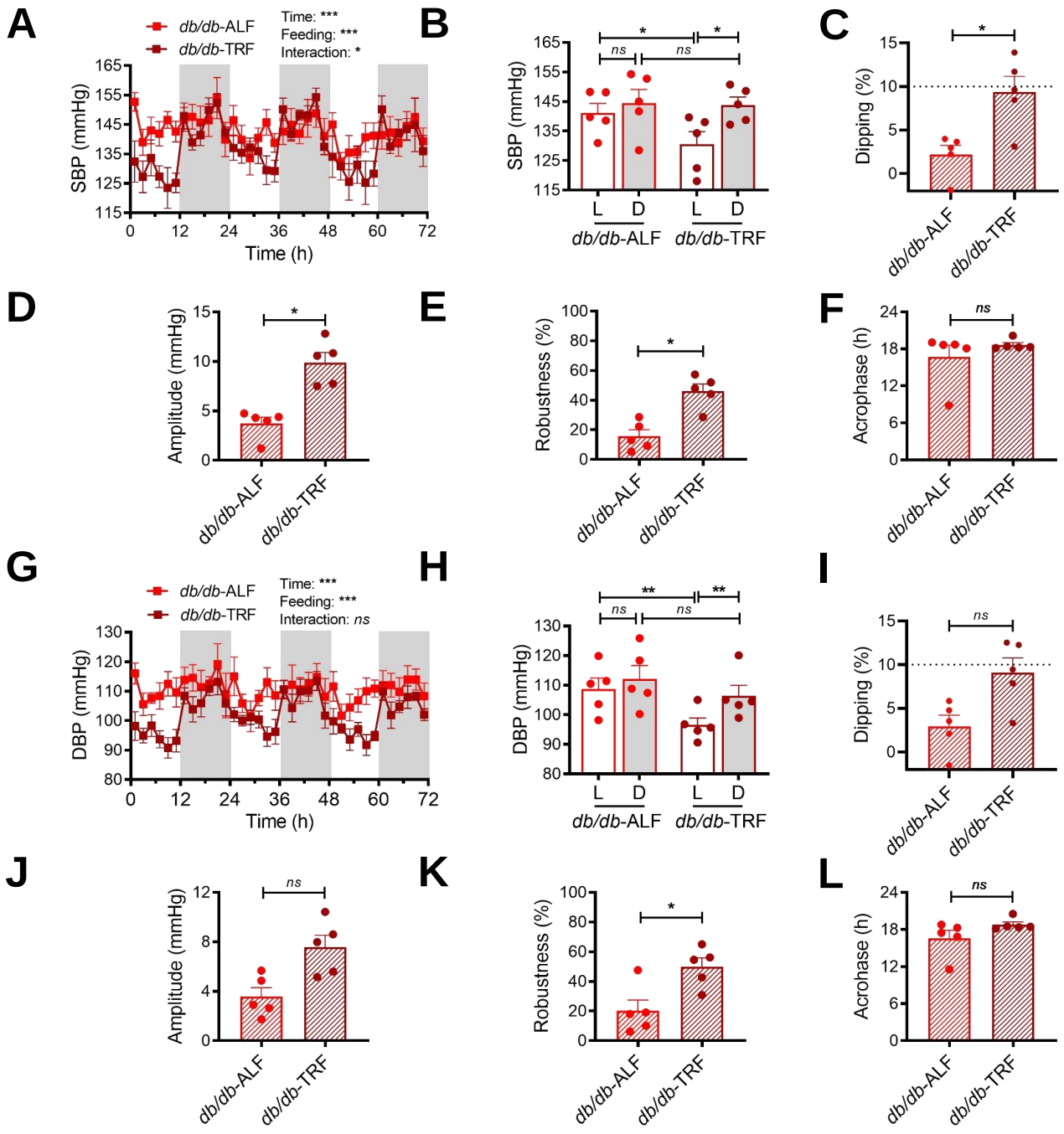

Fig. S4. TRF restores SBP and DBP dipping in the nondipping *db/db* mice. The SBP and DBP data were first collected in 15-week-old *db/db* mice under ALF and then recorded 9 days after 8-h TRF. Five mice in each group. (**A** and **G**) Daily profiles of SBP (A) and DBP (G) in 2-h interval in *db/db*-ALF and *db/db*-TRF mice. The grey box indicates the dark-phase. (**B** and **H**) The 12-hour average SBP (B) and DBP (H) during the light (L) and dark (D) phase. (**C** and **I**) SBP (C) and DBP (I) dipping. The dashed line indicates 10% dipping. (**D** and **J**) Amplitude of the SBP (D) and DBP (J) circadian rhythms. (**E** and **K**) Robustness of the SBP (E) and DBP (K) circadian rhythms. (**F** and **L**) Acrophase of the SBP (F) and DBP (L) circadian rhythms. The data were analyzed by 2-way ANOVA (A, B, G, and H) with multiple comparisons test or paired t-test (C–F and I–L) and were expressed as the mean ± standard error (SEM). *, p<0.05; **, p<0.01; ***, p<0.001; ns, not significant.

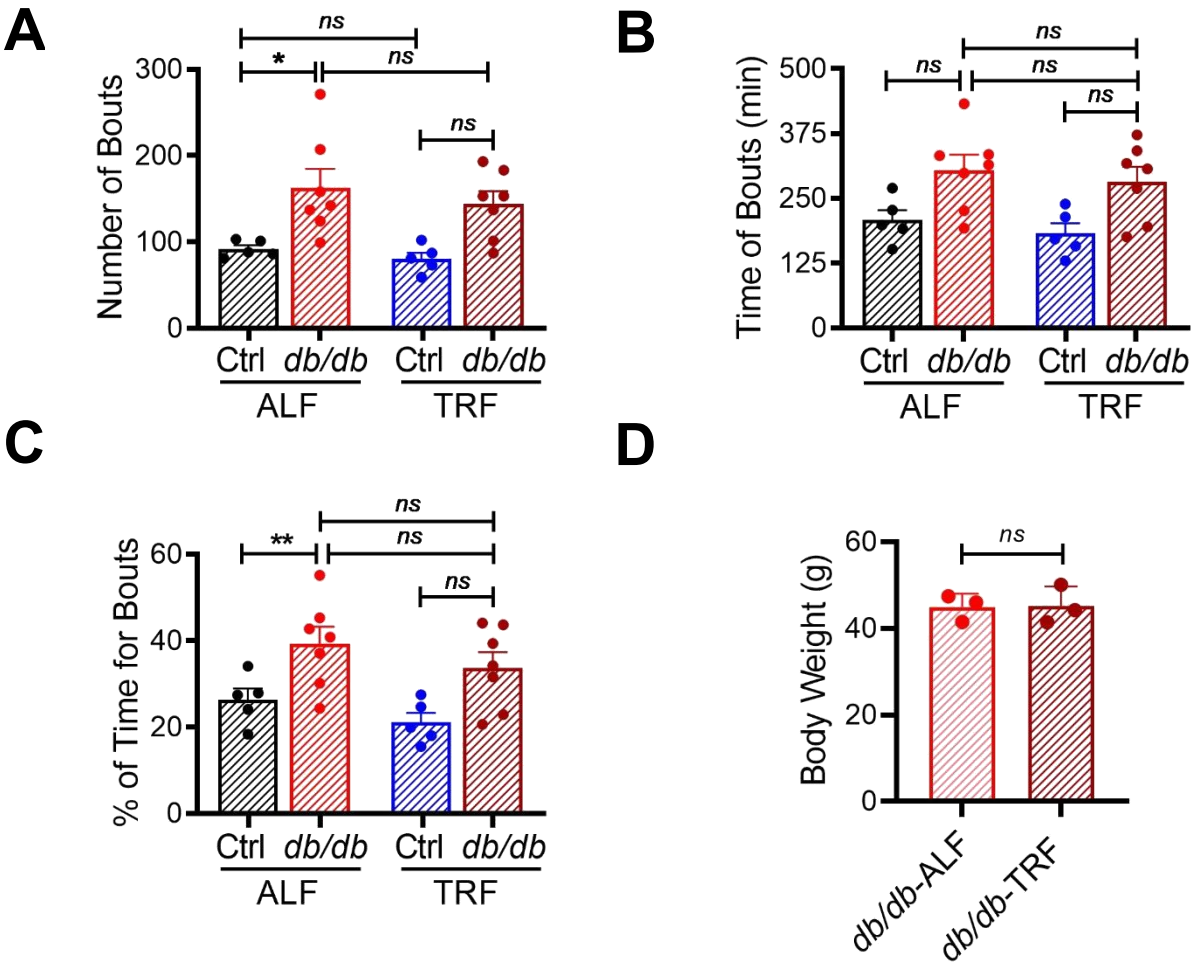

Fig S5. Increasing TRF from 8 h to 12 h does not affect the food intake pattern and body weight in *db/db* mice. Food intake was monitored by BioDAQ in 14-weeks-old *db/db* and control (*db/+*) mice 4 days after 12-hour TRF or ALF. (**A**) Numbers of feeding bouts. (**B**) Duration (time) of feeding bouts. (**C**) Percent of time for feeding bouts. (**D**) Body weight was measured in 14-weeks-old *db/db* 4 days after 12-h TRF or ALF. The data were analyzed by 2-way ANOVA with multiple comparisons test (A–C) and unpaired t-test (D) and were expressed as the mean ± standard error (SEM). *, $p<0.05$; **, $p<0.01$; ns, not significant.

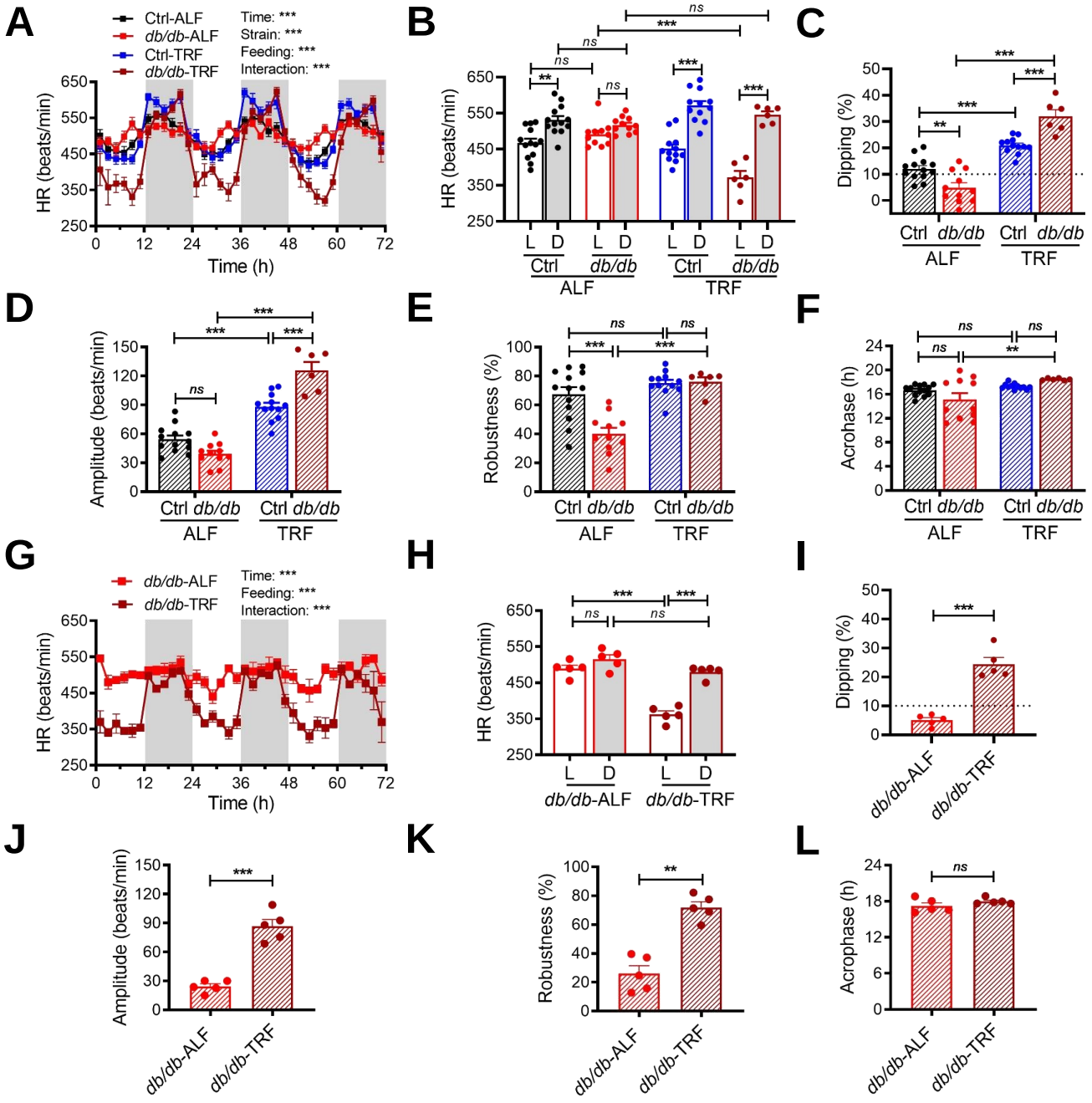

Fig. S6. TRF protects the heart rate (HR) circadian rhythm in *db/db* mice. HR was recorded by telemetry in the 16-week-old *db/db* and control (*db/+*) mice that had been fed ALF or 8-h TRF for 10 weeks (A–F) as well as the 17-week-old *db/db* mice that were fed first ALF and then 9 days after TRF (G–L). (**A** and **G**) Daily profiles of HR in 2-h interval over 72 hours (h). The grey box indicates the dark phase. (**B** and **H**) The 12-h average HR during the light (L) and dark (D) phase. (**C** and **I**) HR dipping (% of HR decrease during the light phase compared to the dark phase). The dashed line indicates 10% dipping. (**D** and **J**) Amplitude of the HR circadian rhythm. (**E** and **K**) Robustness of the HR circadian rhythm. (**F** and **L**) Acrophase of the HR circadian rhythm. The data were analyzed by 3-ANOVA (A and B) and 2-way ANOVA (C–H) with multiple comparisons test or paired t-test (I–L) and were expressed as the mean ± standard error (SEM). *, p<0.05; **, p<0.01; ***, p<0.001; ns, not significant.

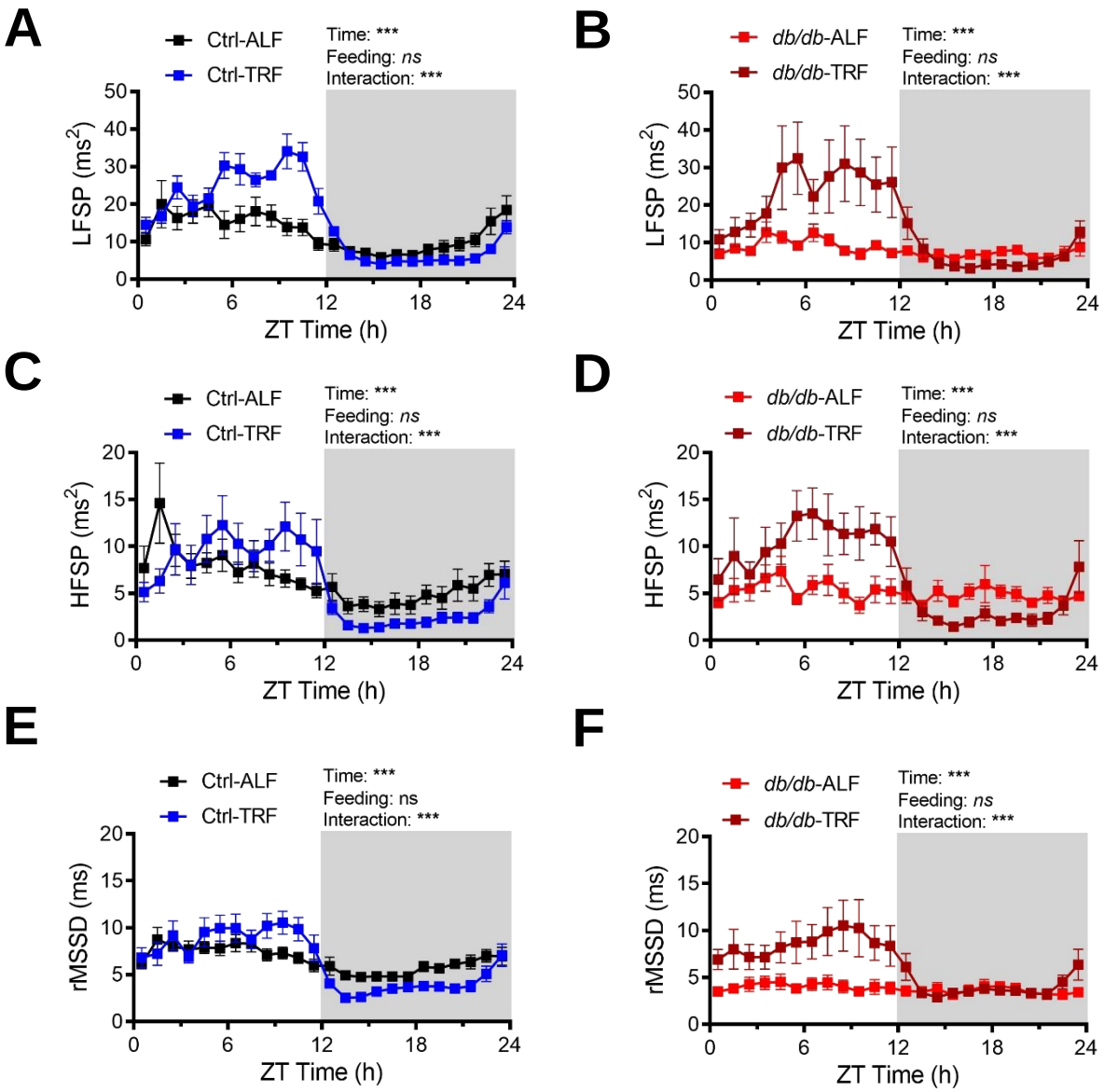

Fig. S7. TRF protects *db/db* mice from the loss of diurnal variation in heart rate variability (HRV). HRV was analyzed by the low-frequency spectral power (LFSP; A and B), high-frequency spectral power (HFSP; C and D), and root mean square of successive RR interval differences (rMSSD; E and F) in the 16-week-old *db/db* and control mice that had been fed ALF or 8-h TRF for 10 weeks. (**A**) Daily profiles of LFSP in 1-h interval over 24 hours (h) in Ctrl-ALF (n=8) and Ctrl-TRF (n=8) mice. (**B**) Daily profiles of LFSP in 1-h interval over 24 hours in *db/db*-ALF (n=8) and *db/db*-TRF (n=6) mice. (**C**) Daily profiles of HFSP in 1-h interval over 24 hours in Ctrl-ALF (n=8) and Ctrl-TRF (n=8) mice. (**D**) Daily profiles of HFSP in 1-h interval over 24 hours in the *db/db*-ALF (n=8) and *db/db*-TRF (n=6) mice. (**E**) Daily profiles of rMSSD in 1-h interval over 24 hours in Ctrl-ALF (n=8) and Ctrl-TRF (n=8) mice. (**F**) Daily profiles of rMSSD in 1-h interval over 24 hours in *db/db*-ALF (n=8) and *db/db*-TRF (n=6) mice. The grey box indicates the dark phase. ZT, zeitgeber time (ZT0 = lights-on and ZT12 = lights-off). The data were analyzed by 2-way ANOVA and were expressed as the mean ± standard error (SEM). ***, p<0.0001; ns, not significant.

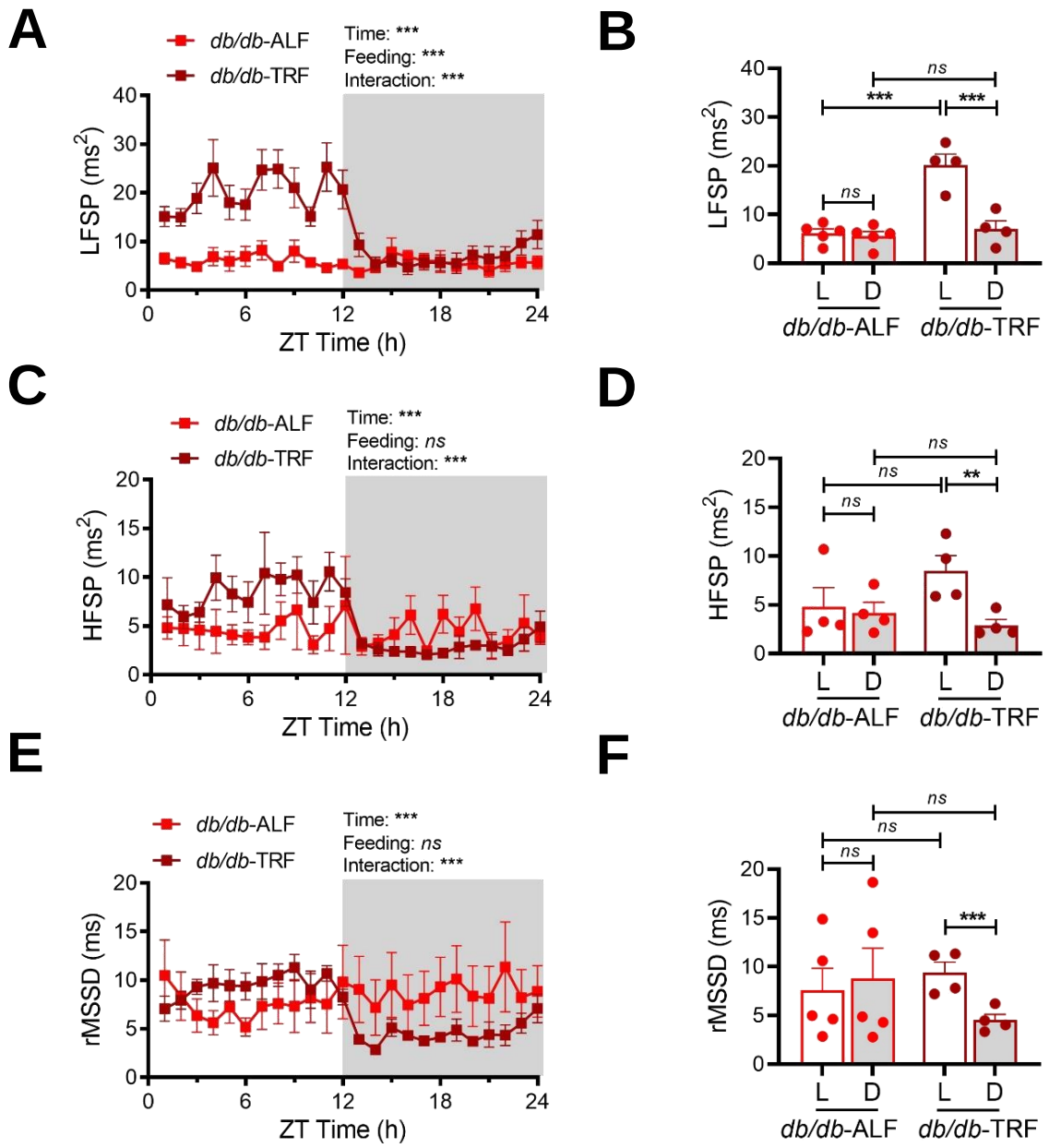

Fig. S8. TRF restores the time-of-day variation of heart rate variability (HRV) in *db/db* mice. HRV was analyzed by the low-frequency spectral power (LFSP; A and B), high-frequency spectral power (HFSP; C and D), and root mean square of successive RR interval differences (rMSSD; E and F) in the 17-week-old *db/db* mice that had been first fed ALF and then 8-h TRF for 9 days. (**A**) Daily profiles of LFSP in 1-h interval over 24 hours in *db/db*-ALF (n=5) and *db/db*-TRF (n=4) mice. (**B**) The 12-h average LFSP during the light (L) and dark (D) phase. (**C**) Daily profiles of HFSP in 1-h interval over 24 hours in *db/db*-ALF (n=4) and *db/db*-TRF (n=4) mice. (**D**) The 12-h average HFSP during the light (L) and dark (D) phase. (**E**) Daily profiles of rMSSD in 1-h interval over 24 hours in *db/db*-ALF (n=5) and *db/db*-TRF (n=4) mice. (**F**) The 12-h average rMSSD during the light (L) and dark (D) phase. The grey box indicates the dark-phase. ZT, zeitgeber time (ZT0 = lights-on and ZT12 = lights-off). The data were analyzed by 2-way ANOVA with multiple comparisons test and were expressed as the mean ± standard error (SEM). ***, p<0.0001; ns, not significant. **. P<0.01; ***, p<0.001; ns, not significant.

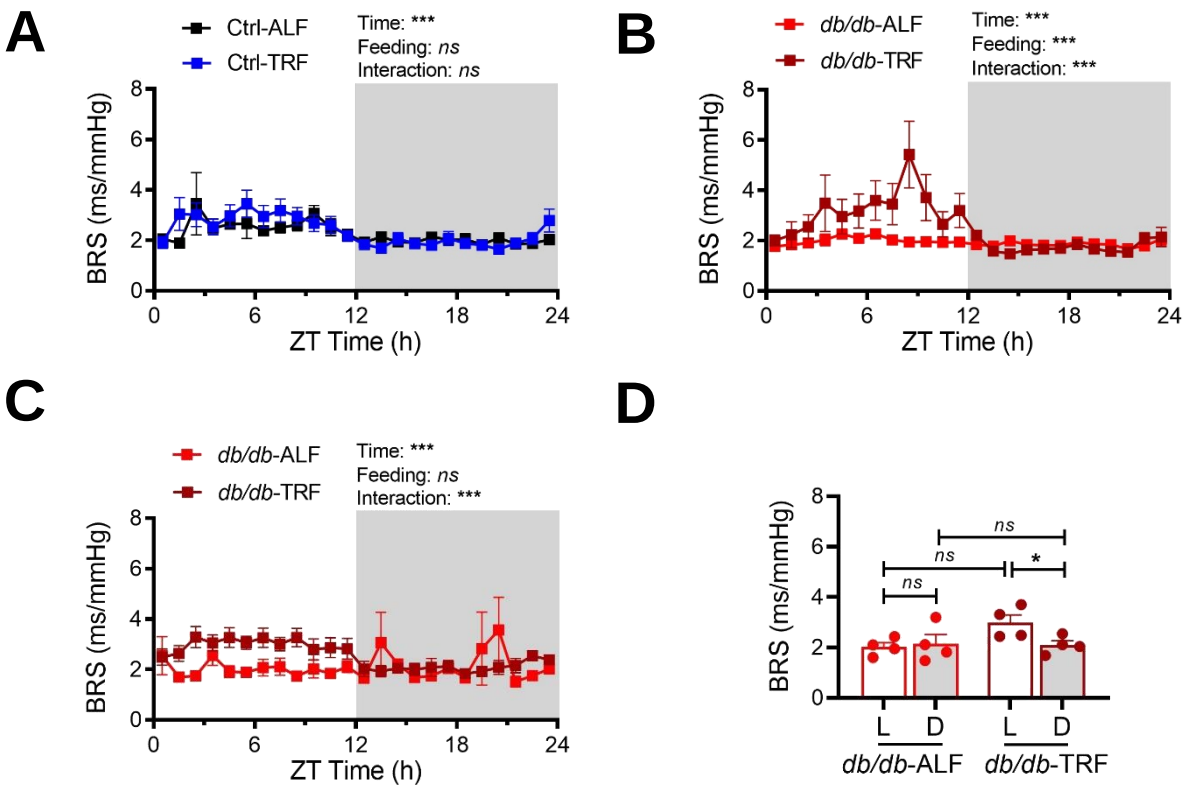

Fig. S9. TRF protects *db/db* mice from the loss of time-of-day variation of spontaneous baroreflex sensitivity. Spontaneous baroreflex sensitivity (BRS) was analyzed in the 16-week-old *db/db* and control (*db/+*) mice that had been fed ALF or 8-h TRF for 10 weeks (A and B) or 17-week-old *db/db* mice that had been fed ALF first and then TRF for 9 days. (**A**) Daily BRS profiles in 1-h interval over 24 hours in Ctrl-ALF (n=4) and Ctrl-TRF (n=5) mice. (**B**) Daily BRS profiles in 1-h interval over 24 hours in *db/db*-ALF (n=10) and *db/db*-TRF (n=6) mice. (**C**) Daily BRS profiles in 1-h interval over 24 hours in *db/db*-ALF (n=4) and *db/db*-TRF (n=4) mice. (**D**) The 12-h average BRS during the light (L) and dark (D) phase in *db/db*-ALF and *db/db*-TRF mice. The grey box indicates the dark-phase. ZT, zeitgeber time (ZT0 = lights-on and ZT12 = lights-off). The data were analyzed by 2-way ANOVA with multiple comparisons test ANOVA and were expressed as the mean ± standard error (SEM). *. P<0.05; ***, p<0.001; ns, not significant.

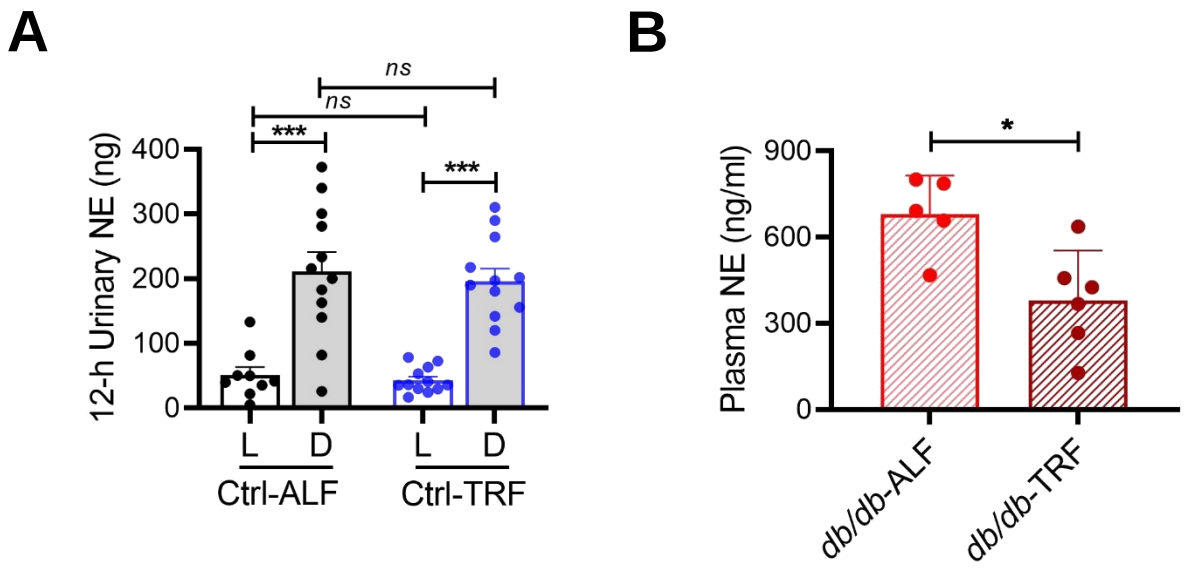

Fig. S10. Effects of TRF on urinary and plasma norepinephrine (NE) in control and *db/db* mice. (**A**) Urinary norepinephrine (NE) in 12-hour (h) urine samples collected during the light (L) and dark (D) phase from the 16-week-old control mice (*db*/+) mice that had been fed ALF or 8-h TRF for 9 days. (**B**) Plasma NE at ZT6 during the light phase from the 16-week-old *db/db* mice that had been fed ALF or 8-h TRF for 7 days. ZT, zeitgeber time (ZT0 = lights-on and ZT12 = lights-off). NE was measured by ELISA. The data were analyzed by 2-way ANOVA with multiple comparisons test (A) and unpaired student t-test (B) and were expressed as the mean ± standard error (SEM). *, $p<0.05$; ***, $p<0.001$; ns, not significant.

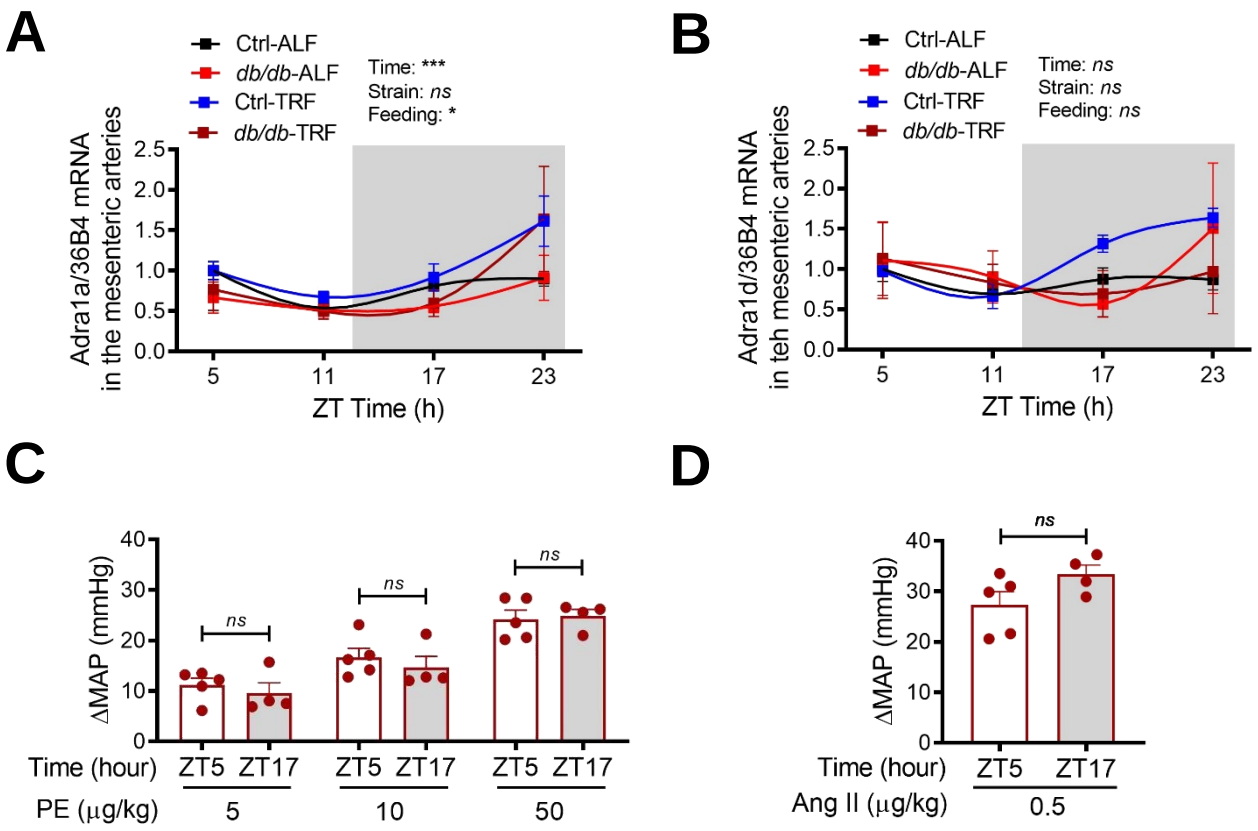

Fig. S11. TRF does not affect the time-of-day variation of vascular reactivity in *db/db* mice. (**A** and **B**) The daily mRNA oscillations of adrenergic receptor α-1a (Adra1a; A) and adrenergic receptor α-1d (Adra1d; B) were determined by real-time PCR in the mesenteric arteries isolated at ZT5, ZT11, ZT17, and ZT23 in 21-week-old *db/db and* control (*db/+*) mice that had been fed ALF or 8-h TRF for 4 weeks. ZT, zeitgeber time (ZT0 = lights-on and ZT12 = lights-off). Adra1a and Adra1d mRNA daily oscillations were normalized to the house-keeping gene 36B4 mRNA and then to the corresponding gene in Ctrl-ALF mice at ZT5. Ctrl-ALF: n=6-7; Ctrl-TRF: n=4-5; *db/db*-ALF: n=4-5, *db/db*-TRF: n=3-5. (**C** and **D**) Eighteen-week-old *db/db* mice were first implanted with telemetry and then fed TRF for 9 days. Under anesthesia conditions, basal MAP was recorded at ZT5 or ZT17 as a baseline. Various phenylephrine concentrations (PE; C) or a single dose of angiotensin II (Ang II; D) were injected at ZT5 or ZT17 via the femoral artery. The instant pressor responses to PE or Ang II were recorded at ZT5 and ZT17. The differences in MAP (ΔMAP) were calculated by subtracting the basal MAP from PE- or Ang II-induced maximal MAP at ZT5 or ZT17. The data were analyzed by 3-way ANOVA with multiple comparisons test (A and B) and paired t-test (C and D) and were expressed as the mean ± standard error (SEM). *, p<0.05; ***, p<0.001; ns, not significant.

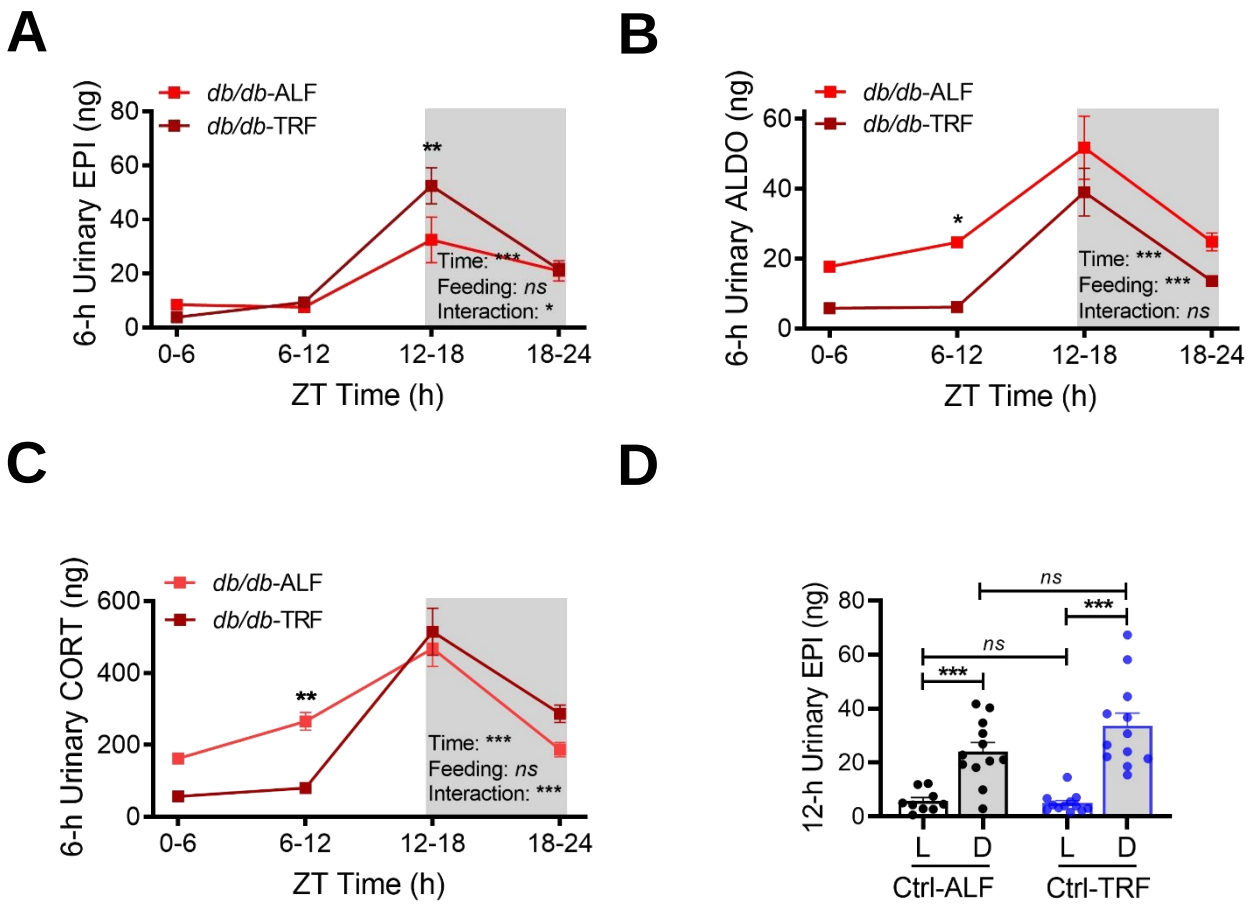

Fig. S12. TRF improves the time-of-day variations in urinary epinephrine (EPI), aldosterone (ALDO), and corticosterone (CORT) in *db/db* mice. (**A**–**C**) Urines were collected every 6 hours within one 24-hour day at ZT0-6, ZT6-12, ZT12-18, and ZT18-24 from 15-week-old *db/db* mice that had been fed ALF or 8-h TRF for 8 weeks. ZT, zeitgeber time (ZT0 = lights-on and ZT12 = lights-off). (**D**) Urinary EPI in 12-h urine samples collected during the light (L) and dark (D) phase from the 16-week-old control mice (*db*/+) mice that had been fed with ALF or 8-h TRF for 9 days. The grey box indicates the dark-phase. The urinary contents of EPI (A and D), ALDO (B), and CORT (C) were measured by ELISA (n=4-5). The data were analyzed by 2-way ANOVA with multiple comparisons test and were expressed as the mean ± standard error (SEM). *, $p<0.05$; **, $p<0.01$; ***, $p<0.001$; ns, not significant.

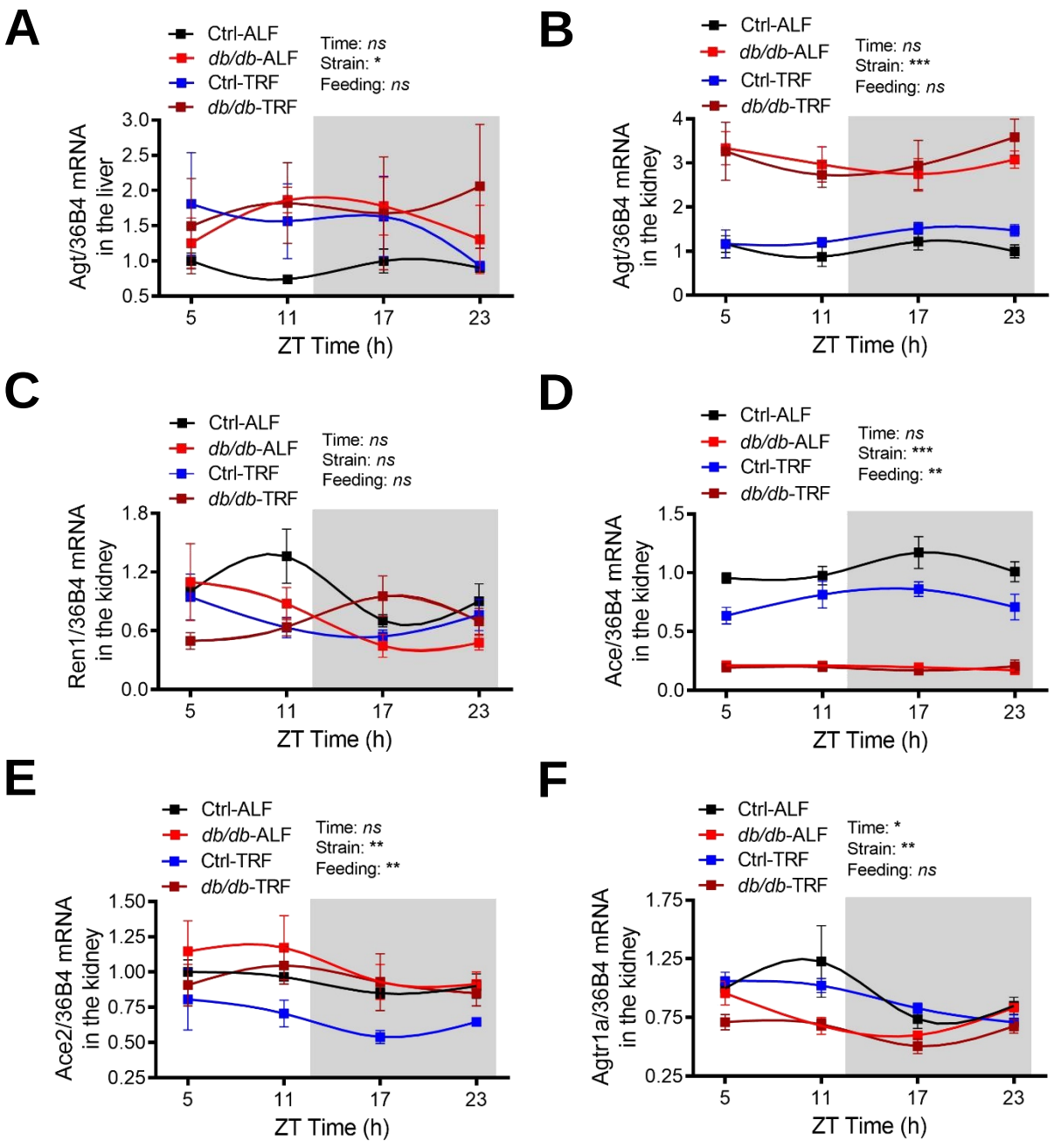

Fig. S13. TRF does not affect the daily mRNA oscillations of Agt, Ren1, Ace1, Ace2, and Agtr1a in the liver or kidney in *db/db* mice. The daily mRNA oscillations of angiotensinogen (Agt) in the liver (**A**) and kidney (**B**), renin (Ren1) in the kidney (**C**), angiotensin-converting enzyme (Ace) in the kidney (**D**), Ace2 in the kidney (**E**), and angiotensin II receptor 1a (Agtr1a) in the kidney (**F**) were determined by real-time PCR at zeitgeber time (ZT)5, ZT11, ZT17 and ZT23 in 21-week-old *db/db and* control (*db/+*) mice that had been fed ALF or 8-h TRF for 4 weeks. The expression of each gene was normalized to the house-keeping gene 36B4 mRNA in the same sample and then normalized to the corresponding gene in Ctrl-ALF mice at ZT5. Ctrl-ALF: n=6-7; Ctrl-TRF: n=4-5; *db/db*-ALF: n=4-5, *db/db*-TRF: n=3-5. The data were analyzed by 3-way ANOVA with multiple comparisons test and were expressed as the mean ± standard error (SEM). *, p<0.05; **, p<0.01; ***, p<0.001; ns, not significant.

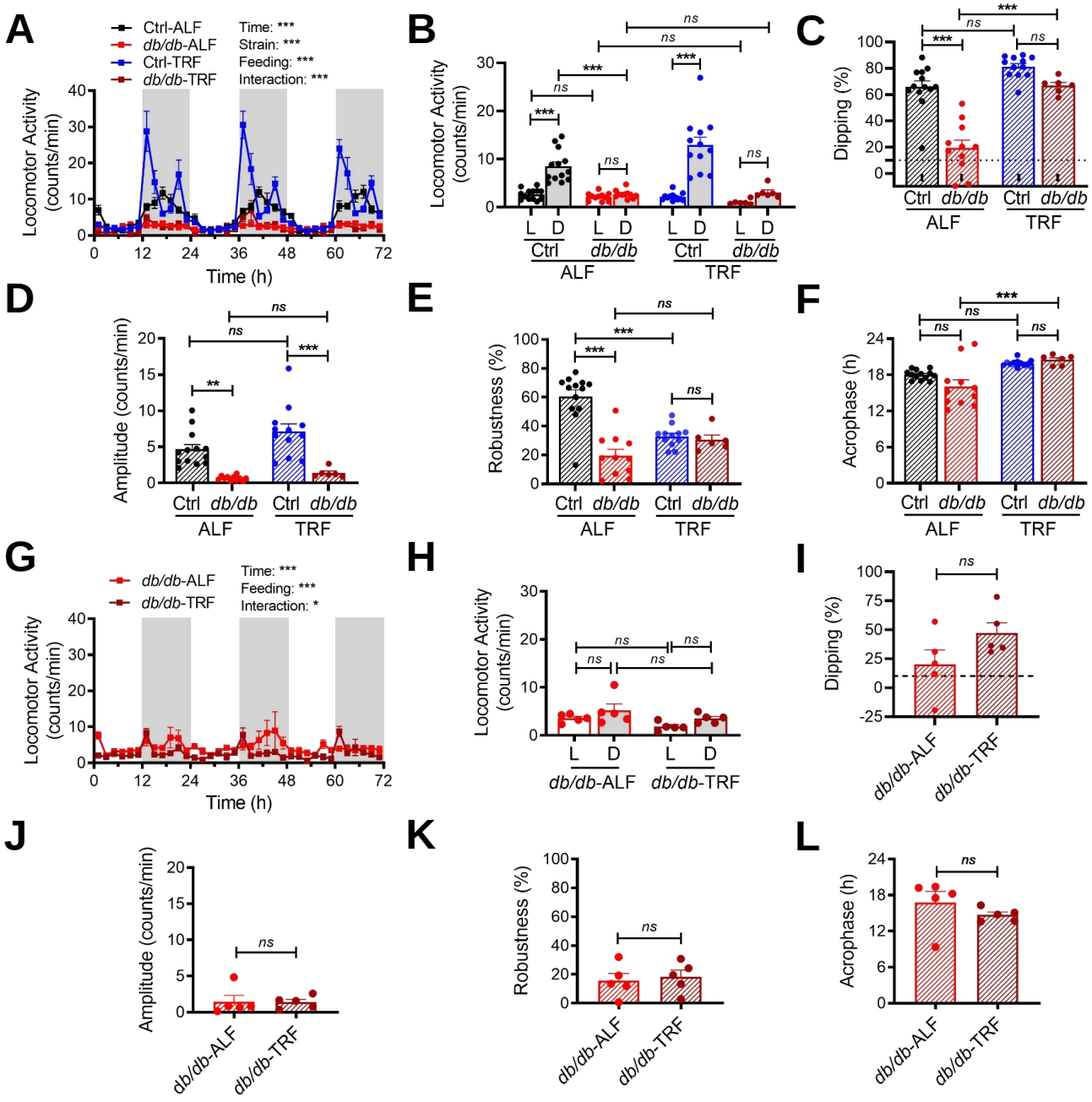

Fig. S14. TRF does not affect locomotor activity circadian rhythm in *db/db* mice. Locomotor activity was recorded by telemetry in the 16-week-old Ctrl-ALF (n=13), *db/db*-ALF (n=11), Ctrl-TRF (n=12), and *db/db*-TRF (n=6) mice that had been fed ALF or 8-h TRF for 10 weeks (A–F) or 15-weeks-old *db/db* mice that had been fed ALF or TRF for 9 days. (**A** and **G**) Daily profiles of the locomotor activity in 2-h intervals over 72 hours (h). The grey box indicates the dark phase. (**B** and **H**) The 12-h average locomotor activity during the light (L) and dark (D) phase. (**C** and **I**) Locomotor activity dipping (% of locomotor activity decreases during the light phase compared to the dark phase). The dashed line indicates 10% dipping. (**D** and **J**) Amplitude of the locomotor activity circadian rhythm. (**E** and **K**) Robustness of the locomotor activity circadian rhythm. (**F** and **L**) Acrophase of the locomotor activity circadian rhythm. The data were analyzed by 3-way ANOVA (A and B) and 2-way ANOVA (C–H) with multiple comparisons test or paired t-test (I–L) and were expressed as the mean ± standard error (SEM). *, p<0.05; **, p<0.01; ***, p<0.001; ns, not significant.

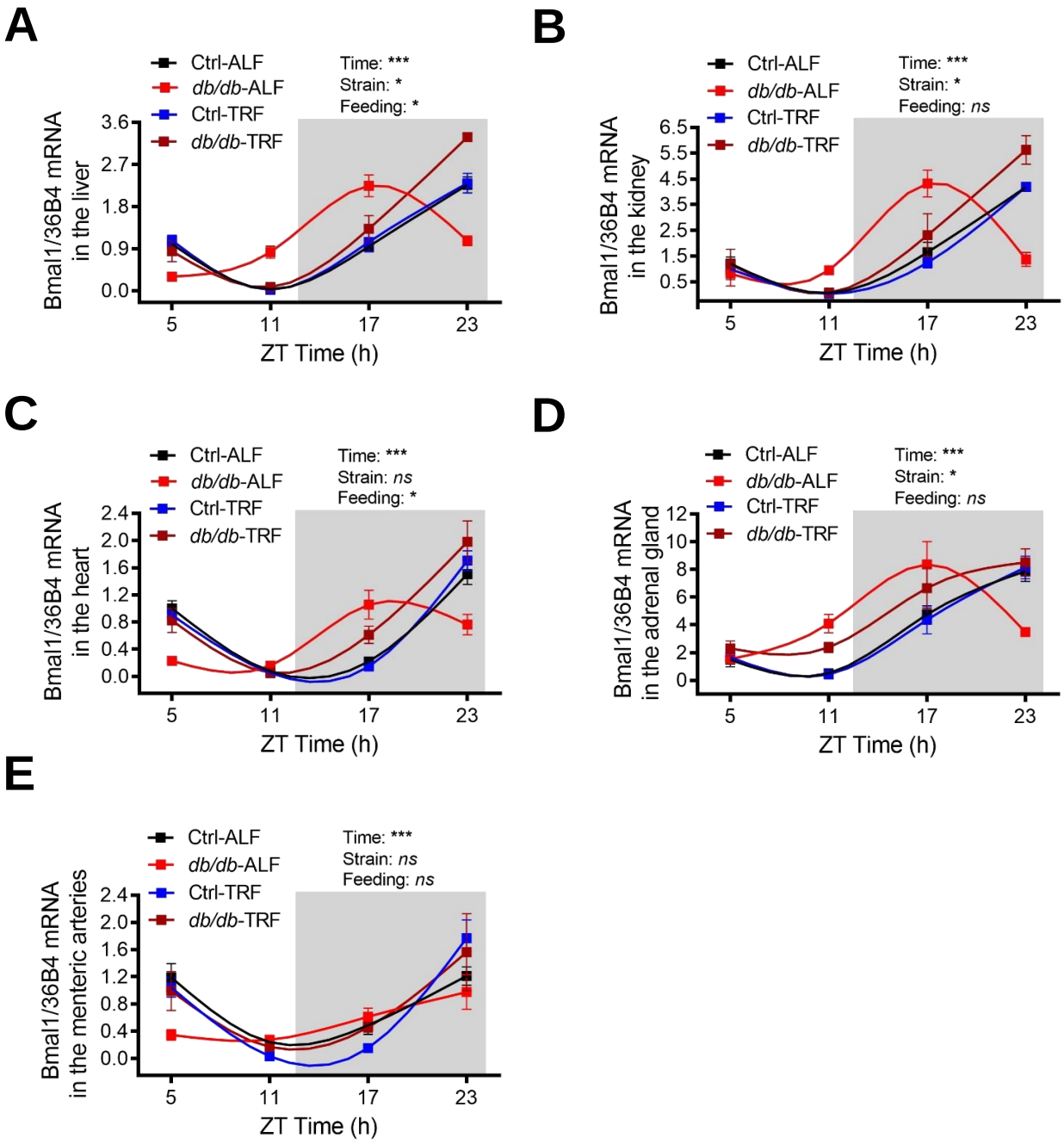

Fig. S15. Effects of TRF on the daily oscillations of Bmal1 gene expression in *db/db* mice. The daily mRNA oscillations of Bmal1 (also known as aryl hydrocarbon receptor nuclear translocator-like [Arntl]) were determined by real-time PCR at ZT5, ZT11, ZT17, and ZT23 in the liver (**A**), kidney (**B**), heart (**C**), adrenal gland (**D**), and mesenteric arteries (**E**) from 21-week-old Ctrl-ALF (n=6-7), Ctrl-TRF (n=4-5), *db/db*-ALF (n=4-5), and *db/db*-TRF (n=3-5) mice that had been fed ALF or 8-h TRF for 4 weeks. ZT, zeitgeber time (ZT0 = lights-on and ZT12 = lights-off). The grey box indicates the dark phase. The daily oscillations of Bmal1 gene expression were normalized to the house-keeping gene 36B4 gene expression and then to the corresponding gene in the Ctrl-ALF mice at ZT5. The data were analyzed by 3-way ANOVA with multiple comparisons test and were expressed as the mean ± standard error (SEM). *, $p<0.05$; ***, $p<0.001$; ns, not significant.

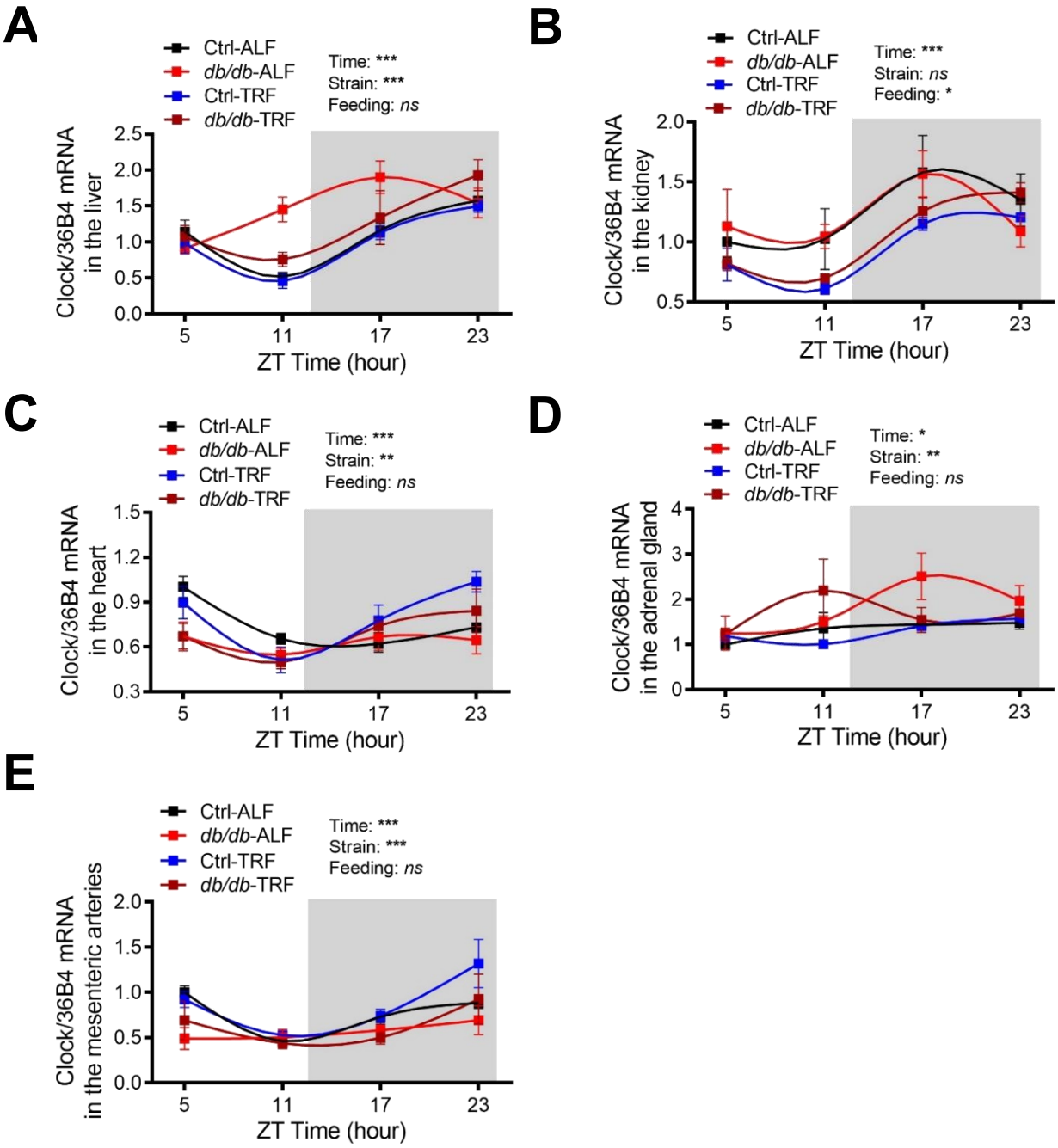

Fig. S16. Effects of TRF on the daily oscillations of Clock gene expression in *db/db* mice. The daily mRNA oscillations of Clock were determined by real-time PCR at ZT5, ZT11, ZT17, and ZT23 in the liver (**A**), kidney (**B**), heart (**C**), adrenal gland (**D**), and mesenteric arteries (**E**) from 21-week-old Ctrl-ALF (n=6-7), Ctrl-TRF (n=4-5), *db/db*-ALF (n=4-5), and *db/db*-TRF (n=3-5) mice that had been fed ALF or 8-h TRF for 4 weeks. ZT, zeitgeber time (ZT0 = lights-on and ZT12 = lights-off). The grey box indicates the dark phase. The daily oscillations of Clock gene expression were normalized to the house-keeping gene 36B4 gene expression and then to the corresponding gene in the Ctrl-ALF mice at ZT5. The data were analyzed by 3-way ANOVA with multiple comparisons test and were expressed as the mean ± standard error (SEM). *, $p<0.05$; **, $p<0.01$; ***, $p<0.001$; ns, not significant.

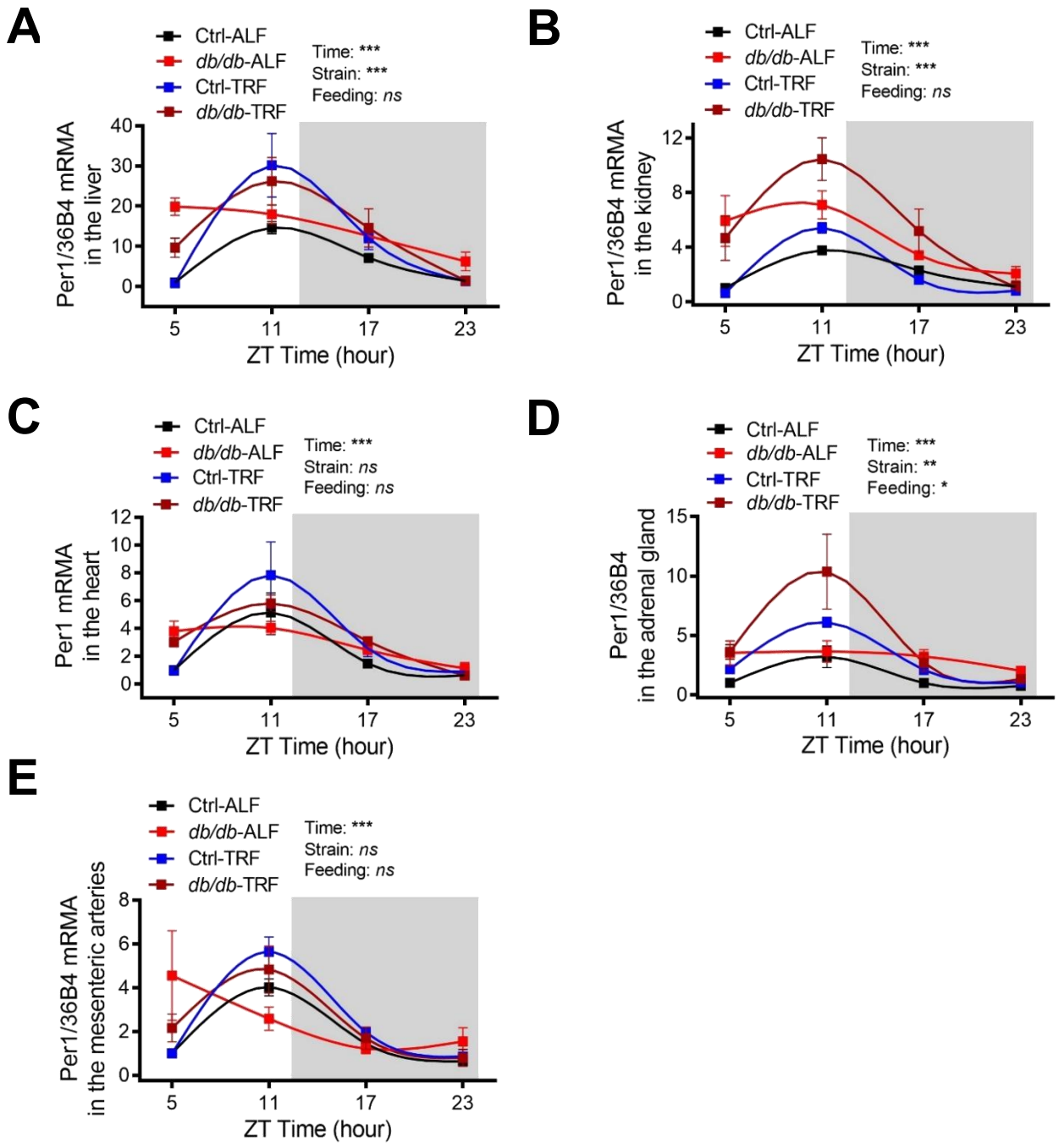

Fig. S17. Effects of TRF on the daily oscillations of Per1 gene expression in *db/db* mice. The daily mRNA oscillations of period 1 (Per1) were determined by real-time PCR at ZT5, ZT11, ZT17, and ZT23 in the liver (**A**), kidney (**B**), heart (**C**), adrenal gland (**D**), and mesenteric arteries (**E**) from 21-week-old Ctrl-ALF (n=6-7), Ctrl-TRF (n=4-5), *db/db*-ALF (n=4-5), and *db/db*-TRF (n=3-5) mice that had been fed ALF or 8-h TRF for 4 weeks. ZT, zeitgeber time (ZT0 = lights-on and ZT12 = lights-off). The grey box indicates the dark phase. The daily oscillations of Per1 gene expression were normalized to the house-keeping gene 36B4 gene expression and then to the corresponding gene in the Ctrl-ALF mice at ZT5. The data were analyzed by 3-way ANOVA with multiple comparisons test and were expressed as the mean ± standard error (SEM). *, $p<0.05$; **, $p<0.01$; ***, $p<0.001$; ns, not significant.

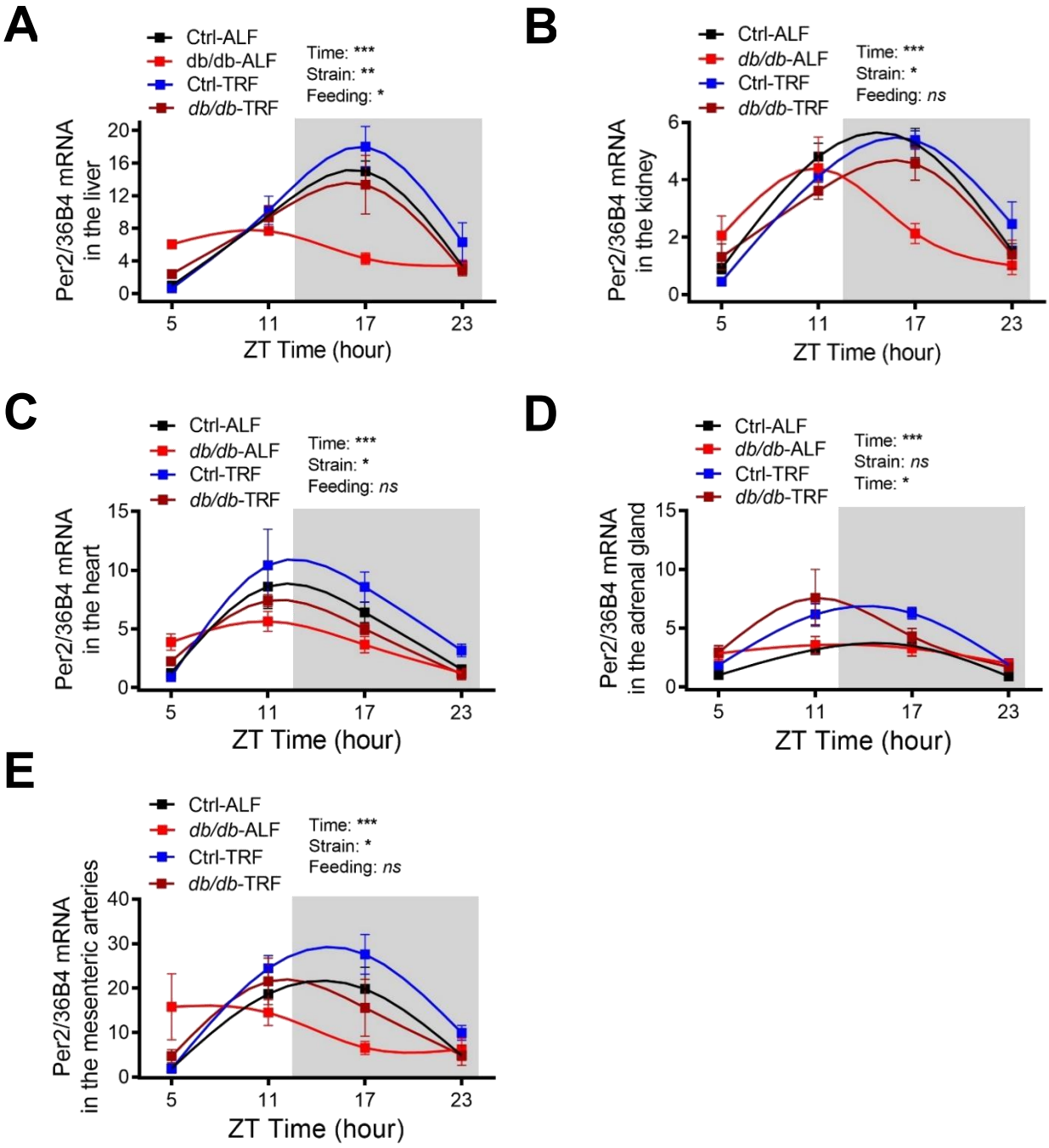

Fig. S18. Effects of TRF on the daily oscillations of Per2 gene expression in *db/db* mice. The daily mRNA oscillations of period 2 (Per2) were determined by real-time PCR at ZT5, ZT11, ZT17, and ZT23 in the liver (**A**), kidney (**B**), heart (**C**), adrenal gland (**D**), and mesenteric arteries (**E**) from 21-week-old Ctrl-ALF (n=6-7), Ctrl-TRF (n=4-5), *db/db*-ALF (n=4-5), and *db/db*-TRF (n=3-5) mice that had been fed ALF or 8-h TRF for 4 weeks. ZT, zeitgeber time (ZT0 = lights-on and ZT12 = lights-off). The grey box indicates the dark phase. The daily oscillations of Per2 gene expression were normalized to the house-keeping gene 36B4 gene expression and then to the corresponding gene in the Ctrl-ALF mice at ZT5. The data were analyzed by 3-way ANOVA with multiple comparisons test and were expressed as the mean ± standard error (SEM). *, $p<0.05$; **, $p<0.01$; ***, $p<0.001$; ns, not significant.

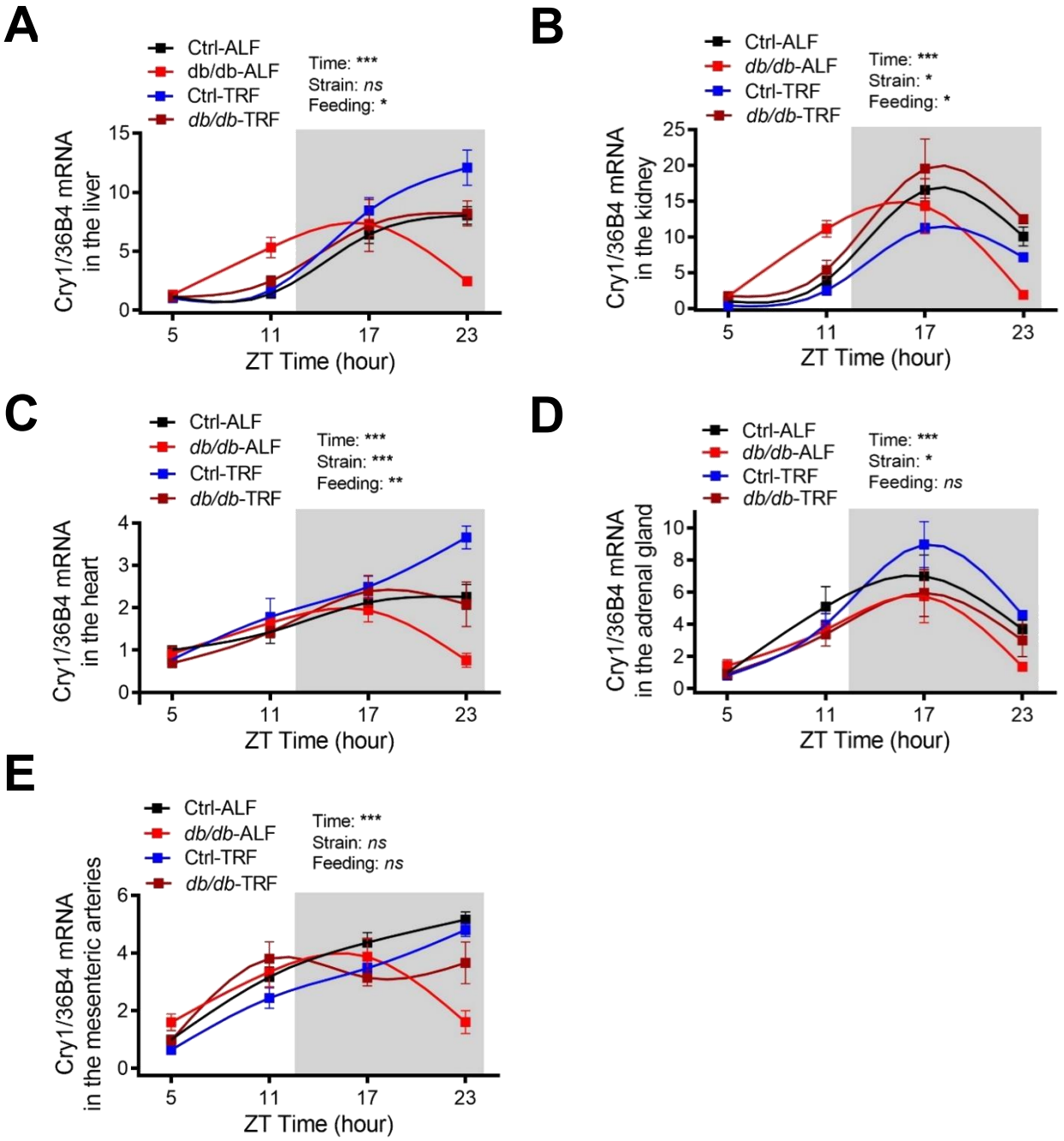

Fig. S19. Effects of TRF on the daily oscillations of Cry1 gene expression in *db/db* mice. The daily mRNA oscillations of cryptochrome 1 (Cry1) were determined by real-time PCR at ZT5, ZT11, ZT17, and ZT23 in the liver (**A**), kidney (**B**), heart (**C**), adrenal gland (**D**), and mesenteric arteries (**E**) from 21-week-old Ctrl-ALF (n=6-7), Ctrl-TRF (n=4-5), *db/db*-ALF (n=4-5), and *db/db*-TRF (n=3-5) mice that had been fed ALF or 8-h TRF for 4 weeks. ZT, zeitgeber time (ZT0 = lights-on and ZT12 = lights-off). The grey box indicates the dark phase. The daily oscillations of Cry1 gene expression were normalized to the house-keeping gene 36B4 gene expression and then to the corresponding gene in the Ctrl-ALF mice at ZT5. The data were analyzed by 3-way ANOVA with multiple comparisons test and were expressed as the mean ± standard error (SEM). *, $p<0.05$; **, $p<0.01$; ***, $p<0.001$; ns, not significant.

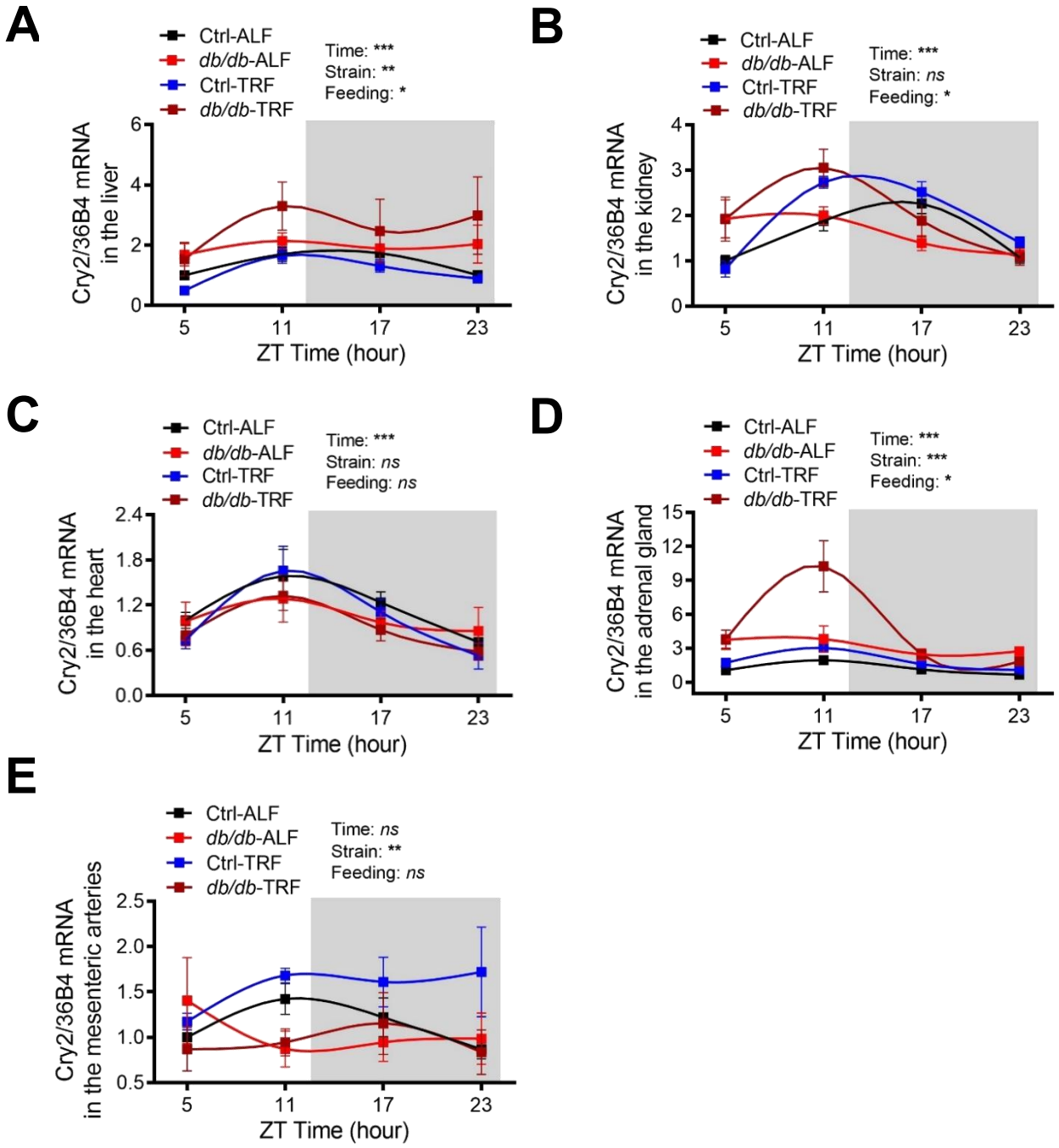

Fig. S20. Effects of TRF on the daily oscillations of Cry2 gene expression in *db/db* mice. The daily mRNA oscillations of cryptochrome 2 (Cry2) were determined by real-time PCR at ZT5, ZT11, ZT17, and ZT23 in the liver (**A**), kidney (**B**), heart (**C**), adrenal gland (**D**), and mesenteric arteries (**E**) from 21-week-old Ctrl-ALF (n=6-7), Ctrl-TRF (n=4-5), *db/db*-ALF (n=4-5), and *db/db*-TRF (n=3-5) mice that had been fed ALF or 8-h TRF for 4 weeks. ZT, zeitgeber time (ZT0 = lights-on and ZT12 = lights-off). The grey box indicates the dark phase. The daily oscillations of Cry2 gene expression were normalized to the house-keeping gene 36B4 gene expression and then to the corresponding gene in the Ctrl-ALF mice at ZT5. The data were analyzed by 3-way ANOVA with multiple comparisons test and were expressed as the mean ± standard error (SEM). *, $p<0.05$; **, $p<0.01$; ***, $p<0.001$; ns, not significant.

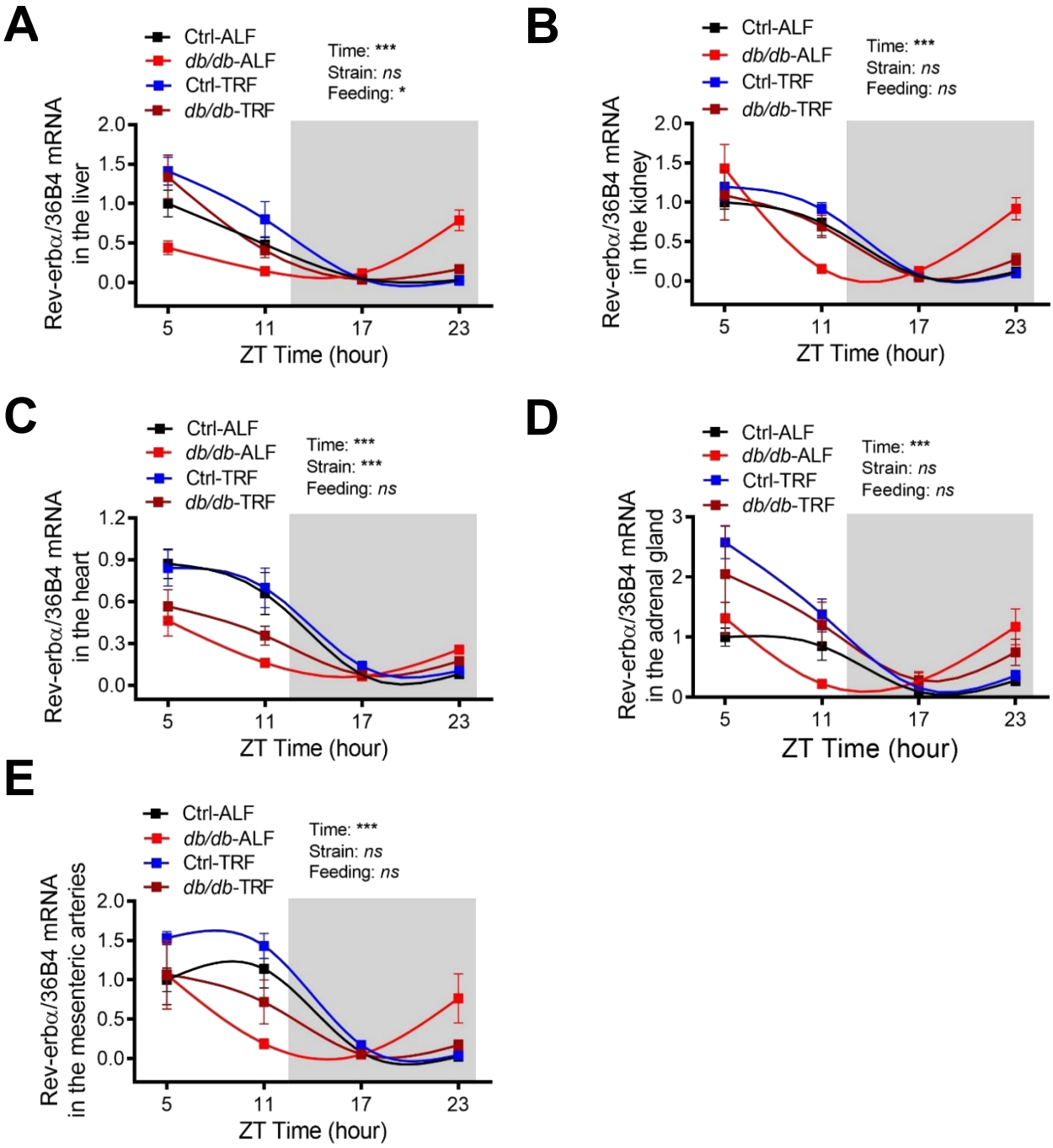

Fig. S21. Effects of TRF on the daily oscillations of Rev-erbα gene expression in *db/db* mice. The daily mRNA oscillations of Rev-erbα (also known as Nr1d1, nuclear receptor subfamily 1, group D, member 1) were determined by real-time PCR at ZT5, ZT11, ZT17, and ZT23 in the liver (**A**), kidney (**B**), heart (**C**), adrenal gland (**D**), and mesenteric arteries (**E**) from 21-week-old Ctrl-ALF (n=6-7), Ctrl-TRF (n=4-5), *db/db*-ALF (n=4-5), and *db/db*-TRF (n=3-5) mice that had been fed ALF or 8-h TRF for 4 weeks. ZT, zeitgeber time (ZT0 = lights-on and ZT12 = lights-off). The grey box indicates the dark phase. The daily oscillations of Rev-erbα gene expression were normalized to the house-keeping gene 36B4 gene expression and then to the corresponding gene in the Ctrl-ALF mice at ZT5. The data were analyzed by 3-way ANOVA with multiple comparisons test and were expressed as the mean ± standard error (SEM). *, $p<0.05$; ***, $p<0.001$; ns, not significant.

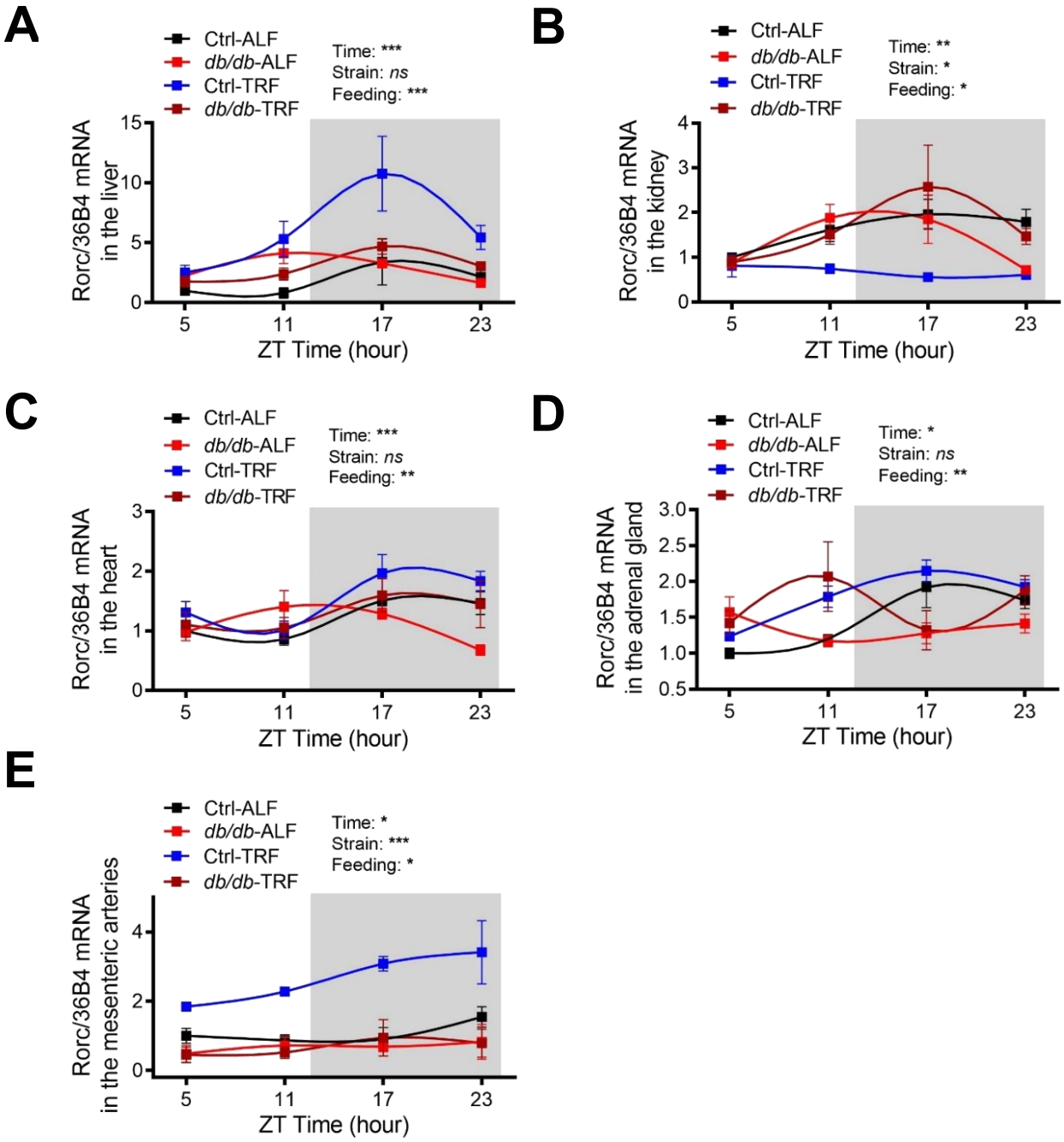

Fig. S22. Effects of TRF on the daily oscillations of Rorc gene expression in *db/db* mice. The daily mRNA oscillations of Rorc (also known as RAR-related orphan receptor gamma) were determined by real-time PCR at ZT5, ZT11, ZT17, and ZT23 in the liver (**A**), kidney (**B**), heart (**C**), adrenal gland (**D**), and mesenteric arteries (**E**) from 21-week-old Ctrl-ALF (n=6-7), Ctrl-TRF (n=4-5), *db/db*-ALF (n=4-5), and *db/db*-TRF (n=3-5) mice that had been fed ALF or 8-h TRF for 4 weeks. ZT, zeitgeber time (ZT0 = lights-on and ZT12 = lights-off). The grey box indicates the dark phase. The daily oscillations of Rorc gene expression were normalized to the house-keeping gene 36B4 gene expression and then to the corresponding gene in the Ctrl-ALF mice at ZT5. The data were analyzed by 3-way ANOVA with multiple comparisons test and were expressed as the mean ± standard error (SEM). *, p<0.05; **, p<0.01; ***, p<0.001; ns, not significant.

Table S1. Real-time PCR primer information

Gene	Primer	Sequence
Bmal1	Forward	5'-ATCAGCGACTTCATGTCTCC-3'
	Reverse	5'-CTCCCTTGCATTCTTGATCC-3'
Clock	Forward	5'-GGCGTTGTTGATTGGACTAGG-3
	Reverse	5'-GAATGGAGTCTCCAACACCCA-3'
Per1	Forward	5’-TCGAAACCAGGACACCTTCTCT-3’
	Reverse	5’-GGGCACCCCGAAACACA-3’
Per2	Forward	5'-AGGCGTCCTTCTTACAGTGAA-3'
	Reverse	5'-CAGGTTGAGGGCATTACCTCC-3'
Cry1	Forward	5'-TCGCCGGCTCTTCCAA-3'
	Reverse	5'-TCAAGACACTGAAGCAAAAATCG-3'
Cry2	Forward	5’-CCTCGTCTGTGGGCATCAA-3’
	Reverse	5’-GCTTTCTTAAGCTTGTGTCCAGATC-3’
Rev-erba	Forward	5'-CCCTGGACTCCAATAACAACACA-3'
	Reverse	5'-GCCATTGGAGCTGTCACTGTAG-3'
Rorc	Forward	5’-TCCACTACGGGGTTATCACCT-3’
	Reverse	5’-AGTAGGCCACATTACACTGCT-3’
Agt	Forward	5’-TCTCTTTACCCCTGCCCTCT-3’
	Reverse	5’-CAGGCAGCTGAGAGAAACCT-3’
Renin	Forward	5’-TCAGGGAGAGTCAAAGGTTTCC-3’
	Reverse	5’-ACAGTGATTCCACCCACAGTCA-3’
Ace	Forward	5’-AGCCCAAGTGTTGTTGAACGA-3’
	Reverse	5’-TGGATACCTCCGTGCTTTTCT-3’
Ace2	Forward	5’-TCCAGACTCCGATCATCAAGC-3’
	Reverse	5’-TGCTCATGGTGTTCAGAATTGT-3’
At1a	Forward	5’-CCAAGAAAGCCATCACCAGATC-3’
	Reverse	5’-TTTCTGGGTTGAGTTGGTCTCA-3’
Adra1a	Forward	5’-ATGAGGAGCCAGGATACGTG-3’
	Reverse	5’-TCTGACTTGTCGGTCTTGAGG-3’
Adra1d	Forward	5’-TCTCCGTAAGGCTGCTCAAG-3’
	Reverse	5’-AACCAGCACAGGACGAAGAC-3’